JOURNAL OF VIROLOGY, Jan. 2003, p. 1524–1539 Vol. 77, No. 2
0022-538X/03/$08.00+0 DOI: 10.1128/JVI.77.2.1524–1539.2003

Kaposi's Sarcoma-Associated Herpesvirus Induces the Phosphatidylinositol 3-Kinase-PKC-ζ-MEK-ERK Signaling Pathway in Target Cells Early during Infection: Implications for Infectivity

Pramod P. Naranatt,[1] Shaw M. Akula,[1] Christopher A. Zien,[2] Harinivas H. Krishnan,[1] and Bala Chandran[1]*

Department of Microbiology, Molecular Genetics and Immunology,[1] and Department of Biochemistry and Molecular Biology,[2] University of Kansas Medical Center, Kansas City, Kansas 66160

Received 2 July 2002/Accepted 11 October 2002

Human herpesvirus 8 (HHV-8) is implicated in the pathogenesis of Kaposi's sarcoma. HHV-8 envelope glycoprotein B (gB) possesses the RGD motif known to interact with integrin molecules, and HHV-8 infectivity was inhibited by RGD peptides, by antibodies against α3 and β1 integrins, and by soluble α3β1 integrin (S. M. Akula, N. P. Pramod, F.-Z. Wang, and B. Chandran, Cell 108:407-419, 2002). Anti-gB antibodies immunoprecipitated the virus α3 and β1 complexes, and virus-binding studies suggest a role for α3β1 in HHV-8 entry. HHV-8 infection induced the integrin-mediated activation of focal adhesion kinase (FAK), implicating a role for integrin and the associated signaling pathways in HHV-8 entry into the target cells. Immediately after infection, target cells exhibited morphological changes and cytoskeletal rearrangements, suggesting the induction of signal pathways. As early as 5 min postinfection, HHV-8 activated the MEK-ERK1/2 pathway. The focal adhesion components phosphatidylinositol 3-kinase (PI 3-kinase) and protein kinase C-ζ (PKC-ζ) were recruited as upstream mediators of the HHV-8-induced ERK pathway. Anti-HHV-8 gB-neutralizing antibodies and soluble α3β1 integrin inhibited the virus-induced signaling pathways. Early kinetics of the cellular signaling pathway and its activation by UV-inactivated HHV-8 suggest a role for virus binding and/or entry but not viral gene expression in this induction. Studies with human α3 integrin-transfected Chinese hamster ovary cells and FAK-negative mouse DU3 cells suggest that the α3β1 integrin and FAK play roles in the HHV-8 mediated signal induction. Inhibitors specific for PI 3-kinase, PKC-ζ, MEK, and ERK significantly reduced the virus infectivity without affecting virus binding to the target cells. Examination of viral DNA entry suggests a role for PI 3-kinase in HHV-8 entry into the target cells and a role for PKC-ζ, MEK, and ERK at a post-viral entry stage of infection. These findings implicate a critical role for integrin-associated mitogenic signaling in HHV-8's infection of target cells and suggest that, by orchestrating the signal cascade, HHV-8 may create an appropriate intracellular environment to facilitate the infection.

Kaposi's sarcoma (KS), seen commonly in human immunodeficiency virus type 1 (HIV-1)-infected AIDS patients, is a highly angiogenic, multicellular tumor with spindle cell proliferation (6). KS-associated herpesvirus (KSHV) or human herpesvirus 8 (HHV-8) genome was first identified in AIDS-KS biopsies (12). In the absence of HIV-1, KS occurs in three epidemiologically distinct forms, and HHV-8 DNA has been detected in all forms of KS (6). Several studies suggest a potential role for HHV-8 in KS pathogenesis (6, 21, 53). HHV-8 is also associated with body cavity-based B-cell lymphomas (BCBL) and multicentric Castleman's disease (53). Cell lines with B-cell characteristics established from the lymphomas carry HHV-8 in a latent form, and a lytic cycle can be induced by 12-*O*-tetradecanoylphorbol-13-acetate (TPA) (53). HHV-8 DNA encodes for more than 80 complete open reading frames (ORFs), which are designated as ORFs 4 to 75 by their homology to ORFs of herpesvirus saimiri, a simian herpesvirus (41, 48). HHV-8 also encodes for more than 20 unique ORFs, which are designated with the prefix K (41, 48).

* Corresponding author. Mailing address: Department of Microbiology, Molecular Genetics and Immunology, The University of Kansas Medical Center, 3901 Rainbow Blvd., Kansas City, KS 66160. Phone: (913) 588-7043. Fax: (913) 588-7295. E-mail: bchandra@kumc.edu.

HHV-8 DNA and transcripts have been identified in vivo in KS spindle and endothelial cells, keratinocytes, epithelial cells, B cells, and macrophages (6). In vitro, HHV-8 has been shown to infect human B, epithelial, endothelial, and foreskin fibroblast (HFF) cells, as well as keratinocytes (11, 46, 61). Although HHV-8 has a broad cellular tropism, analysis of in vitro HHV-8 interaction with host cells and the quantitation of infection has been hampered by the absence of lytic replication by the input virus. In addition, infection is often latent, as evidenced by the presence of circular latent HHV-8 DNA and by the expression of HHV-8 latency-associated nuclear antigen encoded by the ORF 73 gene (61). The γ-1-Epstein-Barr virus (EBV) infection of primary B cells results in latent infection, immortalization of B cells, and consequently maintenance of latent viral episome along with host cell division. In contrast to EBV infection, the infection of primary B cells by HHV-8 does not result in a sustained latent infection and immortalization (unpublished observations). In vitro latent HHV-8 infection in the primary fibroblast or endothelial cells or in the nonadherent B-cell lines is unstable, and the viral DNA is not maintained efficiently and is usually lost in subsequent culturing of the infected cells (unpublished observations).

The identity of receptors utilized by HHV-8 for binding and entry into the host cells, pathways utilized for infection, and

the role of signaling pathways involved in the different stages of viral infection are critical for understanding the molecular basis of HHV-8's role in human diseases. Our studies show that HHV-8 utilizes the ubiquitous cell surface heparan sulfate (HS)-like molecules to bind the target cells (3). HHV-8 encodes for several glycoproteins, and we have demonstrated the interaction of virion envelope-associated HHV-8 glycoprotein B (gB) (ORF 8) and gpK8.1A with HS molecules (2, 64). Our recent studies showed the interaction of HHV-8 gB with the host cell surface α3β1 integrin, and the utilization of α3β1 integrin as one of the cellular receptors for virus entry into the target cells (1). Expression of human α3 integrin increased the infectivity of virus for Chinese hamster ovary (CHO) cells (1). The α3β1 integrin is expressed in vivo in all HHV-8 target cells, implying that distribution of this integrin matches the permissivity for infection (1). Furthermore, HHV-8 infection induced the integrin-mediated activation of $pp125^{FAK}$ (1). These findings implicate a role for α3β1 integrin and the associated signaling pathways in HHV-8 entry into the target cells.

Integrin-ligand interactions lead to a rapid increase in the tyrosine phosphorylation of several cellular proteins, including $pp125^{FAK}$ (22). A number of signaling molecules, including c-Src, $p130^{CAS}$, phospholipase C-γ, phosphatidylinositol 3-kinase (PI 3-kinase), protein kinase C (PKC), and the Ras/Rho family of small GTP-binding proteins have also been identified in focal adhesions. Focal adhesion kinase (FAK) represents a point of convergence from activated integrins and initiates a cascade of intracellular signals that eventually activate the mitogen-activated protein kinase (MAPK) pathways (22). MAPK pathways exist in all eukaryotes and control fundamental cellular processes such as proliferation, differentiation, survival, and apoptosis (30). The basic arrangement of this pathway includes a G-protein working upstream of a core module consisting of three kinases: a MAPK kinase kinase (MAPKKK) that phosphorylates and activates a MAPK kinase (MAPKK), which in turn activates MAPK. Several modes of cross talking between these signaling cascades occur, probably reflecting the necessity to integrate various upstream signals and translate them into appropriate dosed responses (22). Several studies suggest that virus-receptor interactions activate signaling pathways, which not only aid in viral entry into the cells, but also elicit a cellular state that is more receptive for infection (59). Since HHV-8 interacts with integrin α3β1 and induces the phosphorylation of $pp125^{FAK}$ (1), we examined the signaling pathways induced by HHV-8. HHV-8 infection induced cytoskeletal rearrangements at an early stage of infection, suggesting the activation of signaling pathways. HHV-8 infection of target cells leads to the activation of PI 3-kinase and the PKC-ζ isoform, an upstream event leading to the induction of MEK (for MAPK/ERK kinase) and extracellular signal-regulated kinase (ERK). Inhibitors of different kinases significantly reduced virus infectivity, suggesting that by orchestrating the coordinated activation of a PI 3-kinase, PKC-ζ, MEK, and ERK signaling cascade in the target cells, HHV-8 may create an appropriate intracellular environment facilitating infection.

MATERIALS AND METHODS

Cells. HFF cells, human microvascular endothelial dermal (HMVEC-d) cells, 293, recombinant green fluorescent HHV-8 (GFP–HHV-8)-carrying BCBL-1 cells (HHV-8-positive and EBV-negative human B cells (a gift from Jeffrey Vieira, Seattle, Wash.) (61), BJAB cells (HHV-8-negative B cells), CHO-B2 cells transfected with pCDNA3 (CHO-B2/pCDNA) and human α3 integrin cDNA containing pCDNA3 (CHO-B2/clone B3; gifts from J. A. McDonald, Samuel C. Johnson Medical Research Center, Mayo Clinic, Scottsdale, Ariz.) (67), primary mouse embryonic fibroblasts dominant negative (−/−) for FAK (Du3), and control FAK-positive (+/+) Du17 cells (gifts from D. Ilic, University of California at San Francisco) (27) were grown as described previously (2, 27, 67).

Virus. To monitor the HHV-8 binding and entry process, we used the BCBL-1 cells carrying GFP–HHV-8 (61). Expression of GFP is under the control of the promiscuous elongation factor 1–α-promoter. GFP–BCBL-1 cells and control BJAB cells were stimulated with 20 ng of TPA (Sigma)/ml for 6 days. GFP–HHV-8 and [^{3}H]thymidine-labeled HHV-8 in the spent culture medium was concentrated and gradient purified by using Nycodenz (Sigma) as described previously (3). Purity of the virus was also tested by examining the negatively stained virus particles under transmission electron microscope. Only enveloped virus particles were seen in these EM examinations, indicating the purity of virus preparations (3). EM of virus infected target cells showed only enveloped virus particles (3). Purity of the virus was also measured by Western blot reactions with monoclonal antibodies against HHV-8 virion envelope-associated gpK8.1A, gB, and nonstructural ORF 59 proteins. Detection of 75- and 55-kDa polypeptides representing the fully glycosylated heterodimer mature forms of gB and the absence of 110-kDa precursor molecules (2), detection of 68- to 72-kDa polypeptide representing the fully glycosylated mature form of gpK8.1A and the absence of 38-kDa precursor molecules (69), and the absences of ORF 59 were taken as indication for enveloped viruses without contaminating membrane proteins.

GFP–HHV-8 used in our studies is not clonal and contains both wild-type and recombinant viruses. Hence, for each batch of stock virus, virus infectivity was first determined by estimating the green fluorescent cells and then by estimating the HHV-8 ORF 73 protein expressing cells by immunocytochemistry (1), which estimate the total number of infectious particles. GFP–HHV-8 titer was estimated by using HFF and HMVEC-d cell monolayers in eight-well chamber slides (Nalge Nunc International, Naperville, Ill.) (1, 2, 3, 40). After 3 days, slides were examined by a Nikon Eclipse TE300 inverted fluorescent microscope. Green fluorescent cells indicative of GFP–HHV-8 entry and infection were counted by using the Nikon Magna Firewire digital imaging system. After we observed the slides for GFP expressions, cells were fixed with cold acetone and tested with monoclonal anti-ORF 73 antibodies by immunoperoxidase assay (1). The number of cell nuclei positive for ORF 73 staining was counted, and the total number of infectious virus particles per ml of virus stock was calculated. The ratio of infectious GFP–HHV-8 (GFP infectious unit) versus the total infectious virus population (ORF 73 infectious unit [73-IU]) varies from batch to batch and ranged from 1:1 to 1:4. Since we are studying the consequences of enveloped virus binding (both GFP–HHV-8 and wild-type HHV-8) to the target cells, a mixed population does not deter the conclusions drawn from our experiments. Infections were performed at a multiplicity of infection (MOI) of 5 73-IU of HHV-8 per cell. Replication-incompetent HHV-8 was prepared by inactivating HHV-8 with UV light (365 nm) for 20 min at a 10-cm distance. Herpes simplex virus type 2 (HSV-2) was purified by density gradient centrifugation and used at an MOI of 5 per cell. All batches of virus stock and reagents used in the preparations were tested for the presence of endotoxin by using an endpoint chromogenic *Limulus* amebocyte lysate assay as recommended by the manufacturer (Charles River Laboratories, Charleston, S.C.).

Antibodies, substrates, and chemicals. Polyclonal rabbit antibodies immunoprecipitating ERK2 (sc-154), cRaf-1 (sc-227), nPKC-ζ (sc-216), and MEK (sc-219) as active kinases were from Santa Cruz Biotechnology, Inc., Santa Cruz, Calif. Rabbit antibodies detecting the phosphorylated forms of ERK1/2 (Thr202/Tyr204 phospho-p44/42 MAPK), MEK1/2 (Ser217/221 phospho-MEK1/2), cRaf-1(Ser259 phospho-Raf), p38 MAPK (Thr180/Tyr182 phospho-p38 MAPK), and PKC-ζ (Thr410/403 phospho-PKC-ζ) were from Cell Signaling Technology, Beverly, Mass. Wortmannin, phosphatidylinositol-4,5-diphosphate (PIP_2), TPA, bacterial lipopolysaccharide (LPS), lysophosphatidic acid (LPA), sorbitol, and antibodies against β-actin and FAK were from Sigma. A monoclonal antibody detecting phosphotyrosine (PY20) was from Transduction Laboratories, Los Angeles, Calif. Soluble integrin α3β1 and α5β1 (*n*-octyl pyranoside preparation) and polyclonal antibodies against human integrin α3 (CD49c) were from Chemicon International, Temecula, Calif. Anti-rabbit and anti-mouse horseradish peroxidase-, fluorescein isothiocyanate-, or TRITC (tetramethyl rhodamine isothiocyanate)-linked antibodies were from Kirkegaard & Perry Laboratories, Inc., Gaithersburg, Md. Myelin basic protein (MBP) and polyhistidine-tagged MEK were from Upstate Biotechnology and Santa Cruz, respectively. U0126, LY294002, and 12-deoxyphorbol-13-phenylacetate (dPP) were obtained from LC Laboratories, Woburn, Mass. myr-ζ and myr-α/β were from Biosource Interna-

tional, Camarillo, Calif. Tyrosine phosphatase 1B (PTPase 1B) was from Calbiochem, La Jolla, Calif., and protein A-Sepharose CL-4B beads were from Amersham Pharmacia Biotech, Piscataway, N.J.

Rabbit anti-HHV-8 gB antibodies. The production and characterization of rabbit polyclonal antibodies against the baculovirus-expressed purified full-length glutathione *S*-transferase–gB fusion protein have been previously described (2). Immunoglobulin G (IgG) fractions from the sera were purified by protein A-Sepharose 4B columns (Amersham Pharmacia Biotech, Piscataway, N.J.). Nonspecific antibodies were removed by columns of cyanogen bromide-activated Sepharose 4B covalently coupled with purified glutathione *S*-transferase protein and BJAB cell lysate.

Morphological changes and actin polymerization. HFF cells grown on eight-well chamber slides to ca. 75% confluence were serum starved for 24 h and infected with GFP–HHV-8 or mock infected with pelleted supernatants from TPA-induced BJAB cells or incubated with medium containing fetal bovine serum (HyClone) or LPA at 37°C. At various times, cells were washed, fixed with 3.7% formaldehyde in phosphate-buffered saline (PBS) for 10 min, washed, permeabilized by 0.1% Triton X-100 in PBS for 3 min, washed again, and incubated with 1% bovine serum albumin in PBS to block the nonspecific binding sites. These cells were incubated for 20 min at room temperature with rhodamine-labeled phalloidin (Molecular Probes, Eugene, Oreg.) in PBS, washed, and then examined under a fluorescence microscope.

Immune-complex kinase assays. Target cells grown to 70 to 80% confluence in 25-cm^2 flasks were serum starved for 24 h, cooled to 4°C, and infected with GFP–HHV-8 at 37°C. Cells were also incubated with kinase inhibitors (U0126, wortmannin, LY294002, and PKC-ζ inhibitory peptides) for 1 h at 37°C and infected with GFP–HHV-8 at 37°C in the presence of inhibitors. Anti-gB antibodies or soluble integrins were incubated with HHV-8 for 1 h at 37°C before infection of the cells. At different time points, cells were rinsed twice with ice-cold PBS and lysed for 20 min on ice with lysis buffer (20 mM Tris-HCl, pH 7.4; 137 mM NaCl; 10% glycerol; 1% Triton X-100; 25 mM β-glycerophosphate; 2 mM EDTA; 20 mM sodium pyrophosphate; 5 μg of aprotinin/ml; 5 μg of leupeptin/ml; 1 mM sodium orthovanadate [Na_3VO_4], 5 mM banzamidine, 1 mM phenylmethylsulfonyl fluoride). Cell lysates were centrifuged at 13,000 × *g* for 15 min at 4°C, and supernatants were collected. The protein concentration was measured by using the BCA protein assay (Pierce, Rockford, Ill.), adjusted to equal amounts of protein, and immunoprecipitated with respective antibodies and protein A-Sepharose beads. Immune complexes were washed five times with lysis buffer and twice with kinase buffer (10 mM $MgCl_2$; 25 mM β-glycerophosphate; 25 mM HEPES, pH 7.5; 5 mM benzamidine; 0.5 mM dithiothreitol; 1 mM Na_3VO_4) and then incubated with 2 μCi of [γ-^{32}P]ATP (Perkin-Elmer) and 5 μg of substrate (MBP for ERK and PKC-ζ, MEK for Raf-1) in the kinase buffer for 20 min at 30°C. Reactions were stopped by adding 2× sample buffer and analyzed by sodium dodecyl sulfate–12% polyacrylamide gel electrophoresis (SDS–12% PAGE). Phosphorylated substrate was detected by PhosphorImager analyses (Molecular Dynamics, Sunnyvale, Calif.) and by autoradiography. Bands were scanned, and the band intensities were assessed by using the ImageQuant software program (Molecular Dynamics).

PI 3-kinase assay. Cell lysates were immunoprecipitated with PY20 antibody, and the beads were washed twice with lysis buffer (0.05 M Tris, pH 7.4; 0.15 M NaCl; 1% Nonidet P-40; 1 mM phenylmethylsulfonyl fluoride; 5 μg of leupeptin/ml; 5 μg of pepstatin/ml; 1 mM Na_3VO_4; 10 mM NaF) with 0.5 M LiCl and 0.5 M NaCl and once with kinase buffer (20 mM Tris-HCl, pH 7.5; 100 mM NaCl; 0.5 mM EDTA; and protease inhibitors). PI 3-kinase activity was assessed by incubating the beads in 50 μl of kinase buffer containing 20 μg of PIP_2 for 10 min at room temperature before the addition of 200 μM $MgCl_2$, 20 μM ATP, and 10 μCi of [γ-^{32}P]ATP for 15 min. The product, phosphatidylinositol-3,4,5-trisphosphate (PIP_3) was extracted with chloroform–methanol–1 N HCl (1:1:1), dried completely, resuspended in 50 μl of chloroform-methanol (1:1), spotted onto thin-layer chromatography plates (Whatman LK6D), and resolved in an isopropanol–2 M acetic acid (4:1) solvent system. PIP_3 was detected by autoradiography and quantitated. To test the specificity, phosphotyrosine residues in PI 3-kinase were dephosphorylated by incubating the immunoprecipitates with 0.5 U of PTPase 1B for 2 h at 30°C before assaying for PI 3-kinase activity.

Western blot. Total lysates (10 μg) or equal volume of immune-complex bound protein A-Sepharose beads were resolved by SDS–10% PAGE, transferred to nitrocellulose membranes, and immunobloted with anti-phospho antibodies recognizing only the activated form of proteins. To confirm equal protein loading, blots were also reacted with antibodies detecting the respective total protein or β-actin. Immunoreactive bands were developed by enhanced chemiluminescence reaction (Perkin-Elmer), visualized by autoradiography, and quantitated.

Neutralization of GFP–HHV-8 infectivity. The ability of LY294002, wortmannin, myr-ζ, myr-α/β, and U0126 to neutralize GFP–HHV-8 infectivity was tested as described before (40). Briefly, cells were incubated with different concentrations of specific inhibitors at 37°C for 1 h with Dulbecco modified Eagle medium (DMEM) and then infected with GFP–HHV-8 at 37°C for 2 h in the presence of inhibitors. Cells were washed and incubated 37°C with growth medium for 3 days. Cells were also transfected for 48 h with ERK antisense oligonucleotide (AS-1/2; 5′-GCCGCCGCCGCCGCCAT-3′) and the scrambled control (SC-1/2; 5′-GG CCCGCTCGCGCACCC-3′) before GFP–HHV-8 infection. After 3 days, green fluorescent cells were examined under a fluorescence microscope and counted by using the Nikon Magna Firewire digital imaging system (40). After examination for GFP expression, cells were fixed with acetone and examined for HHV-8 ORF 73 protein by immunoperoxidase staining as described earlier (1).

Cytotoxicity assay. DMEM containing different concentrations of various inhibitors were incubated with HFF cells for 4 h or 4 days. At different time points, supernatants were collected and assessed for the cellular toxicity by using a cytotoxicity assay kit (Promega).

Blocking of HHV-8 binding. [^{3}H]thymidine-labeled density gradient-purified HHV-8 (5,000 cpm) (3) was incubated in medium alone or in medium with 10 μg of heparin or chondroitin sulfate A/ml for 90 min at 4°C. These mixtures were added to Du17 and Du3 cells and then incubated for 90 min at 4°C. To test whether different kinase inhibitors prevent the binding of virus or entry into target cells, HFF cells were preincubated with various inhibitors before addition of the radiolabeled HHV-8. After incubation, cells were washed five times and lysed with 1% SDS and 1% Triton X-100, radioactivity precipitated with trichloroacetic acid, and counted.

IFA. Surface immunofluorescence assay (IFA) with 0.1% paraformaldehyde-fixed cells and IFA with acetone-fixed cells were done as described previously (2).

Internalization of HHV-8 DNA. The effect of kinase inhibitors on HHV-8 internalization was assessed by PCR detecting the internalized HHV-8 DNA as described earlier (35), with minor modifications. Briefly, untreated HFF cells or HFF cells incubated with kinase inhibitors for 1 h at 37°C were infected with GFP–HHV-8 at an MOI of 5 73-IU per cell. After 2 h of incubation with virus, cells were washed twice with PBS to remove the unbound virus. Cells were treated with trypsin-EDTA for 5 min at 37°C to remove the bound noninternalized virus. Detached cells were washed twice to remove the virus and trypsin-EDTA. Cells were pelleted, and total DNA from the cells and from the stock virus was isolated by using DNeasy kit (Qiagen, Valencia, Calif.) and subjected to semiquantitative PCR analysis according to the method of Koelle et al. (29). Isolated DNA was quantitated by UV spectrophotometer, and serial 10-fold dilutions (500 to 0.5 ng) were subjected to PCR in standard cocktail containing the primers ORF25(F) (5′-CGA GAT AAT TCC CAC GCC G-3′) and ORF25(R) (5′-GTG CCA TGA CTA GCC AAC-3′). A standard was prepared by cloning the ORF 25 PCR product into the pGEM-T vector (Promega) and quantitated. Log_{10} dilutions of copy standards (10^6 to 1^1 copies) were amplified in parallel by using the same PCR master mix. The PCR products (637 bp) were resolved on a 1.2% agarose gel and visualized by ethidium bromide staining. The intensity of the bands was measured by using ImageQuant (Molecular Dynamics), and the copy number of internalized HHV-8 DNA was calculated against the standard curve. The authenticity of the PCR product was confirmed by hybridization with digoxigenin-labeled internal oligonucleotide ORF 25 probe.

RESULTS

HHV-8 induces the polymerization of actin and morphological changes in the target cells. One of the hallmarks of integrin interaction with ligands is the reorganization and remodeling of actin cytoskeleton, which are controlled by the Rho family of small GTPases, such as Rho, Rac, and cdc42 (22, 24). Activated cdc42 induces the formation of filopodia, thin finger-like extensions containing actin bundles. Rac regulates the formation of lamellipodia or ruffles, curtain-like extensions often formed along the edge of the cell. Rho mediates the formation of stress fibers, elongated actin bundles that traverse the cells and promote cell attachment to the extracellular matrix through Fas (43). These GTPases are activated by lipid kinase, PI 3-kinase, upon FAK and c-Src phosphorylation and converge their effect on focal adhesion assembly through actin

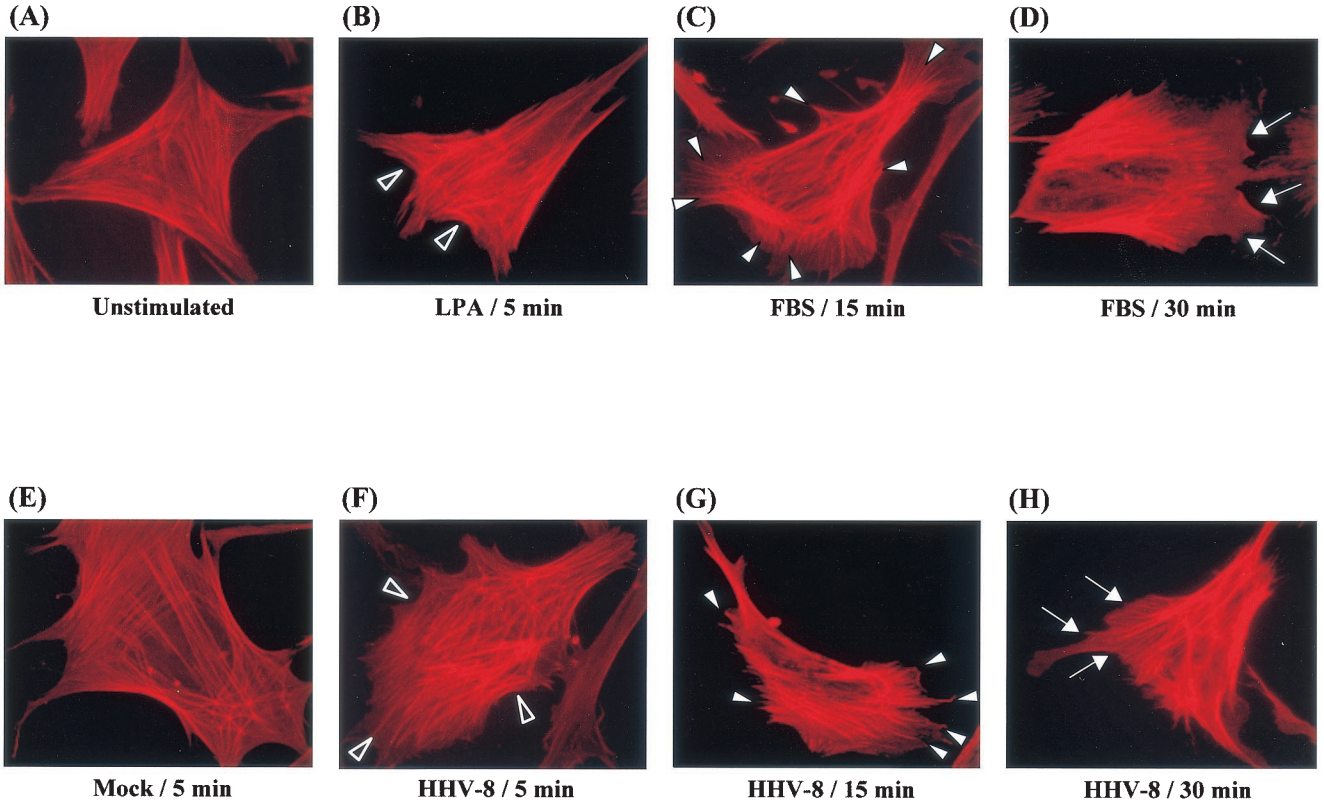

FIG. 1. HHV-8–target cell interaction induces the actin cytoskeleton reorganization. Serum-starved HFF cells incubated with different ligands at 37°C were collected at various time points, fixed, permeabilized, and stained for polymerized actin by rhodamine-labeled phalloidin for 20 min at room temperature. (A) Unstimulated control cells; (B) cells incubated with 20 ng of LPA/ml for 5 min; (C and D) cells incubated with DMEM with 10% FBS for 15 and 30 min, respectively; (E) cells mock infected for 5 min; (F, G, and H) cells infected with GFP–HHV-8 for 5, 15, and 30 min, respectively. Open arrowheads indicate accumulated actin stress fibers. Closed arrowheads indicate hair-like membrane filopodia extensions. Arrows indicate sites of membrane ruffling.

micro filament reorganization and MAPK signaling pathways (22).

While studying HHV-8 infection, we observed the following characteristic morphological changes in the infected target cells. Serum-starved unstimulated (Fig. 1A) and mock-infected (Fig. 1E) HFF cells exhibited strong peripheral F-actin staining along the cell edges, which is indicative of cortical actin fibers. The cell surface margins were well defined and smooth. Within 5 min after infection, HHV-8 induced the rapid polymerization of actin in HFF cells, leading to an increase in the accumulation of stress fibers within the cell (Fig. 1F). These HHV-8-induced changes were comparable to the effects observed in HFF cells 5 min after treatment with 20 ng of LPA/ml (Fig. 1B). The HHV-8-induced increase in the F-actin content was associated with the formation of filopodia extensions on the surface of HFF cells within 15 min postinfection (Fig. 1G). By about 30 min postinfection, cellular ruffling was noticed (Fig. 1H). The HHV-8-induced appearance of filopodia and lamellipodia mimicked the effect of 10% fetal bovine serum (FBS) on the serum-starved HFF cells at 15 min (Fig. 1C) and 30 min (Fig. 1D), respectively. These results demonstrated the modulation of actin polymerization, leading to cellular morphological changes and thus indicating the induction of signaling cascade early during HHV-8 infection.

HHV-8 interaction with α3β1 induces PI 3-kinase activity during the early stage of infection. PI 3-kinase is important as a downstream effector of FAK, which is activated either directly or through Src kinase via Ras (22). PI 3-kinase is a member of a family of lipid kinases consisting of a p85 regulatory subunit and a p110 catalytic subunit. The p85 subunit of PI 3-kinase binds directly to the phosphorylated FAK. The products of PI 3-kinase activation, phosphatidylinositol-3,4-bisphosphate and PIP_3, are increased in the plasma membrane of activated but not in quiescent cells and act as second messengers for a number of cell functions. Phosphorylation of PI 3-kinase is one of the early signaling events of integrin-ligand interaction, and the morphological changes induced by Rho, Rac, and cdc42 activation are downstream effects of such PI 3-kinase activation (22, 24, 31). Since we observed the prototypical morphological changes of integrin ligation by HHV-8 infection, we first examined whether HHV-8 induces the PI 3-kinase pathway. Infected cell lysates were immunoprecipitated with PY20 phosphotyrosine antibodies, and PI 3-kinase activity was quantitated by using PIP_2 as a substrate (Fig. 2A, lanes 1 to 7, and B). As controls for these assays, cells were mock infected with pelleted supernatants from TPA-induced HHV-8-negative BJAB cells or treated with DMEM containing 20% FBS (Fig. 2). As early as 5 min postinfection, PI

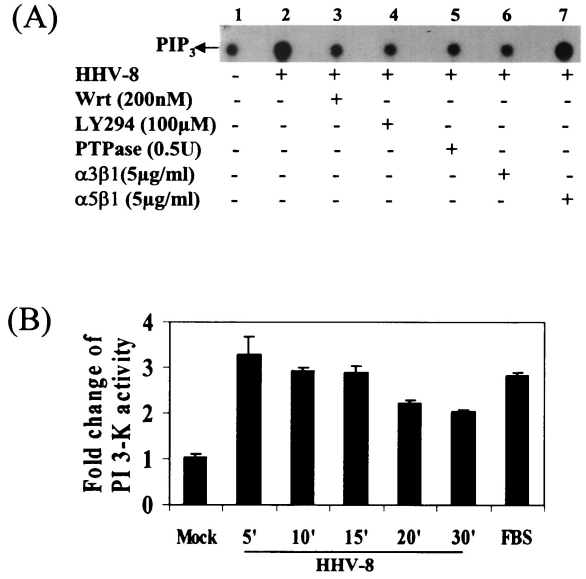

FIG. 2. HHV-8 activates PI 3-kinase in the target cells via its interactions with α3β1 integrin. (A) Induction of PI 3-kinase by HHV-8. Serum-starved HFF cells were mock infected (lane 1) or infected with HHV-8 (lane 2) for 5 min. Cells were also preincubated with the PI 3-kinase inhibitors wortmannin or LY294002 for 1 h at 37°C and then infected with virus in the presence of inhibitors for 5 min (lanes 3 and 4). The phosphotyrosine residue in PI 3-kinase was dephosphorylated by incubating the immunoprecipitates with 0.5 U of PTPase 1B for 2 h at 30°C before an assay for PI 3-kinase activity (lane 5) was carried out. Virus was also preincubated with 5 μg of soluble α3β1 or α5β1/ml for 1 h at 37°C before infection of the cells (lanes 6 and 7). Equal protein concentrations of cell lysates were immunoprecipitated with PY20 antibodies, assayed for PI 3-kinase activity by using sonicated PIP_2 as the substrate, and resolved with radiolabeled PIP_3 by ascending thin-layer chromatography, and PIP_3 spots were detected by autoradiography. (B) Kinetics and quantitation of PI 3-kinase activity induced by HHV-8. Serum-starved HFF cells were mock infected for 15 min or infected with HHV-8 for the indicated time points or treated with FBS for 15 min and assayed for PI 3-kinase activity as described in Fig. 2A. Radioactive PIP_3 spots were quantitated and expressed as fold change of PI 3-kinase activity over mock-infected cells.

3-kinase activity in the infected cells increased to two- to threefold over the mock-infected cells, was sustained for up to 15 min, and decreased thereafter (Fig. 2B). To ascertain the specificity of PI 3-kinase induced by HHV-8, HFF cells were preincubated for 1 h at 37°C with various PI 3-kinase inhibitors, infected with virus for 5 min in the presence of inhibitors, and assayed for PI 3-kinase activities (Fig. 2A). About 95% of the HHV-8-induced PI 3-kinase activity was inhibited by 200 nM wortmannin (Fig. 2A, lane 3), a PI 3-kinase inhibitor binding covalently to the p110 catalytic subunit of PI 3-kinase. Similarly, 99% of HHV-8-induced PI 3-kinase activation was inhibited by 100 μM LY294002 (Fig. 2A, lane 4), a mechanistically distinct inhibitor that competes with ATP for binding to the p110 subunit of PI 3-kinase (63). When the immunoprecipitates were treated with 0.5 U of PTPase 1B, HHV-8-induced PI 3-kinase phosphorylation was lowered by 94% (Fig. 2A, lane 5), thus demonstrating the specificity of these reactions. These results demonstrated that HHV-8 induced PI 3-kinase activation in the target cells early during infection.

HHV-8's interaction with α3β1 integrin (1) and the induction of PI 3-kinase in the target cells prompted us to examine the role of HHV-8–α3β1 interaction in the PI 3-kinase activation. HHV-8 was preincubated with 5 μg of soluble α3β1 or α5β1 integrins/ml for 1 h at 37°C. HFF cells were infected with the mixtures for 5 min and assayed for PI 3-kinase activity. As shown in Fig. 2A, lanes 6 and 7, incubation of virus with α3β1 reduced the PI 3-kinase activation by 96%, and no effect was seen with α5β1 treatment. These results not only demonstrated the specificity of PI 3-kinase induction by HHV-8 but also suggested that HHV-8 interactions with α3β1 is critical for the PI 3-kinase induction observed in the infected cells.

HHV-8 activates MAPK-ERK during the early stage of infection. Since one of the downstream effects of integrin-PI 3-kinase–Rho GTPase activation is the regulation of MAPK pathways (14, 47), we next examined whether HHV-8 induces the ERK pathway. Lysates from HFF cells infected with HHV-8 for different time points were analyzed for ERK activity in an in vitro immune-complex kinase assay, after immunoprecipitation of ERK2/1 by anti-ERK2 antibodies. For controls, cells were mock infected, treated with DMEM containing 20% FBS, or infected with HSV-2. Quanitation of ^{32}P-labeled MBP (Fig. 3A, top panel) as a measure of ERK activity showed that, compared to mock infection (Fig. 3A, lane 1), HHV-8 infection induced a marginal increase in ERK phosphorylation as early as 5 min (Fig. 3A, lane 2), and a two- and threefold increase at 10 and 15 min postinfection, respectively (Fig. 3A, lanes 3 and 4). This activation reached a maximum of 5-fold by 30 min (Fig. 3A, lane 5) and dropped at 60 min to 1.5-fold (Fig. 3A, lane 6). No further increase in stimulation was detected at 2, 4 and 6 h postinfection (data not shown). FBS used as a positive control induced a rapid activation of ERK in 15 min (Fig. 3A, top panel, lane 7). In contrast, similar to the previous findings (36), HSV-2 infection had no effect on ERK activity even after 60 min postinfection (Fig. 3A, top panel, lane 8). Western blot analysis of HHV-8-infected cell lysates with anti-phospho-ERK1/2 (phospho-p44/42 MAPK) antibodies demonstrated an increase in the phosphorylated forms of ERK1/2 with kinetics similar to the kinase assay (Fig. 3A, middle panel), thus confirming the induction of ERK activity. A steady increase in HHV-8-induced ERK activation was seen, which reached a peak activity of fourfold at 30 min postinfection (Fig. 3A, middle panel). Equal amounts of ERK being immunoprecipitated (data not shown) or equal loading of total lysate between the treatments were confirmed by Western blot reactions with antibodies against the total ERK2 protein (Fig. 3A, lower panel). These results also demonstrated the steady-state level of endogenous ERK2 and suggested that HHV-8 infection was activating the endogenous or preexisting ERK.

To determine whether the HHV-8–ERK activation is a cell type-specific phenomenon, ERK1/2 induction was tested in HMVEC-d cells with phosphorylation-specific antibodies (Fig. 3C). Compared to HFF cells, the endogenous level of phospho-ERK1/2 in HMVEC-d cells is much lower (Fig. 3C, top panel, lane 1). Similar to HFF cells, compared to mock infection (Fig. 3C, lane 1), HHV-8 induced a threefold increase in ERK phosphorylation as early as 5 min (Fig. 3C, lane 2), which increased to fourfold by 10 min (Fig. 3C, lane 3), attaining a maximal activation of sixfold at 15 min postinfection (Fig. 3C, lane 4). The HHV-8-induced ERK activity dropped to fourfold at 30 min (Fig. 3C, lane 5) and reached the basal level by 60

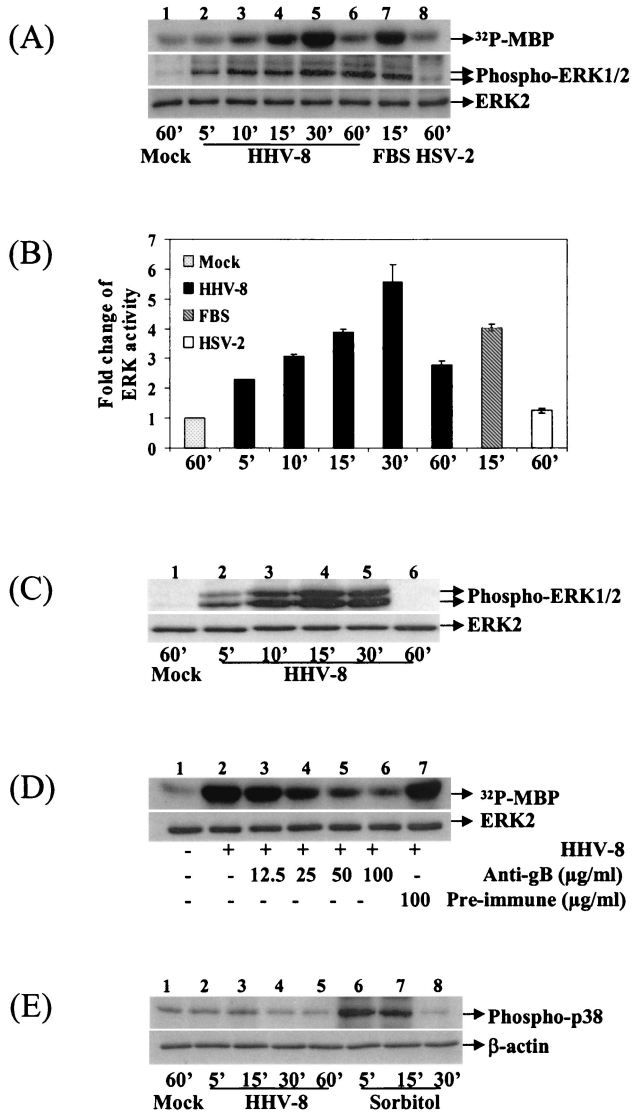

FIG. 3. Activation of MAPK-ERK1/2 by HHV-8 during early times postinfection. (A) Kinetics of MAPK-ERK1/2 induction in HFF cells by HHV-8. Serum-starved HFF cells were either mock infected (lane 1), infected with HHV-8 for different time points (lanes 2 to 6), treated with DMEM containing 20% FBS for 15 min (lane 7), or infected with HSV-2 at an MOI of 5 for 60 min (lane 8). Equal protein concentrations of cell lysates were immunoprecipitated with anti-ERK antibodies, and immune complexes were incubated with [γ-^{32}P]ATP and MBP for 20 min at 30°C, boiled in sample buffer, and analyzed by SDS–12% PAGE. A portion of the lysate was resolved by SDS–10% PAGE and subjected to Western analysis with anti-phospho-ERK1/2 antibodies (middle panel). Equal total lysate being resolved is shown by probing with anti-ERK2 antibodies (bottom panel). The bands were scanned, and intensities were assessed. (B) Quantitation of ERK activity induced by HHV-8. ^{32}P-labeled MBP bands were quantitated, and the ERK activity in mock-infected HFF cells was considered as "1" for comparison to infected cells. (C) Kinetics of ERK1/2 induction in HMVEC-d cells. In the top panel, serum-starved HMVEC-d cells were either mock infected (lane 1) or infected with HHV-8 for different time points (lanes 2 to 6). Cell lysates were resolved by SDS-PAGE and Western blotted with anti-phospho-ERK1/2 antibodies. Membranes were then stripped and reprobed with anti-ERK2 antibodies (bottom panel). (D) Inhibition of ERK induction by HHV-8 neutralizing antibodies. Serum-starved HFF cells were mock infected (lane 1) or infected with HHV-8 (lane 2), with virus preincubated with different concentrations of rabbit anti-HHV-8 gB IgG antibodies (lanes 3 to 6) or preimmune IgG antibodies (lane 7) for 30 min. Lysates were subjected to a kinase assay (top panel) or immunoprecipitate was Western blotted with ERK2 antibodies (bottom panel) as described in the Fig. 3A legend. (E) HHV-8 activates MAPK-ERK1/2 but not p38-MAPK. Serum-starved HFF cells were mock infected, infected with HHV-8, or treated 0.5 M sorbitol for the indicated times. Cell lysates were tested with anti-phospho p38-MAPK antibodies (top panel) or with anti-β actin antibodies (lower panel).

min postinfection (Fig. 3C, lane 6). The total ERK2 levels remained the same during the infection (Fig. 3C, bottom panel). Similar kinetics of ERKl/2 induction were observed in human kidney epithelial cells (293) (data not shown), suggesting the universal nature of HHV-8-mediated signaling and the activation of ERK1/2.

To determine whether HHV-8 gene expression is needed for ERK activation, replication-incompetent GFP–HHV-8 was prepared by UV irradiation. After 20 min of UV exposure, HHV-8 was unable to establish infection in HFF cells, as measured by GFP-expressing cells and by staining for ORF 73 protein; however, binding of [^{3}H]thymidine-labeled HHV-8 to HFF cells was not affected (data not shown). In cells incubated with UV light-exposed HHV-8, two- and fourfold ERK1/2 activations, as measured by phospho-ERK1/2 antibodies, were seen at 15 and 30 min postinfection, respectively (data not shown). This result suggested that ERK activation of HHV-8 was probably not dependent on HHV-8 gene expression.

Specificity of ERK1/2 activity induced by HHV-8. We have previously shown that the rabbit antibodies raised against a recombinant HHV-8 envelope glycoprotein gB neutralized the infectivity of HHV-8 by ca. 80% at 60-μg/ml concentrations by blocking virus entry into the cells without affecting the virus binding (2). We have also shown that HHV-8 gB interacts with the $\alpha 3\beta 1$ integrin and activated FAK phosphorylation (1). At 100-μg/ml concentrations, these antibodies also inhibited ca. 75% of HHV-8-induced FAK phosphorylation (1). To confirm that we were detecting ERK1/2 induction driven by HHV-8, HHV-8 was preincubated with rabbit anti-HHV-8 gB IgG antibodies or with preimmune control IgG antibodies for 1 h at 37°C before HFF cells were infected. Incubation of HHV-8 with anti-gB antibodies reduced the ERK1/2 induction at 30 min postinfection in a dose-dependent manner (Fig. 3D, top panel, lanes 3 to 6). No inhibition was seen with preimmune IgG antibodies (Fig. 3D, lane 7). Quanitation of ^{32}P-labeled MBP (Fig. 3D, top panel) demonstrated that anti-gB antibodies at 12.5-, 25-, 50-, and 100-μg/ml concentrations reduced the HHV-8-induced ERK activity at 30 min postinfection by 16, 46, 82, and 88%, respectively. Western blot analyses of immune complexes detected equal amounts of total ERK2 protein, thus demonstrating that equal ERK were immunoprecipitated (Fig. 3D, bottom panel). Further, all of the reagents used in the preparation of virus stocks were free of bacterial LPS, as tested by *Limulus* amebocyte lysate assay (data not shown). These results demonstrated that ERK was specifically induced by HHV-8 infection and not by the contaminating host cell factors and/or LPS.

To determine whether HHV-8 infection activates other MAPK pathways, phosphorylation-specific antibodies were used to examine the induction of LPS–stress-activated p38-

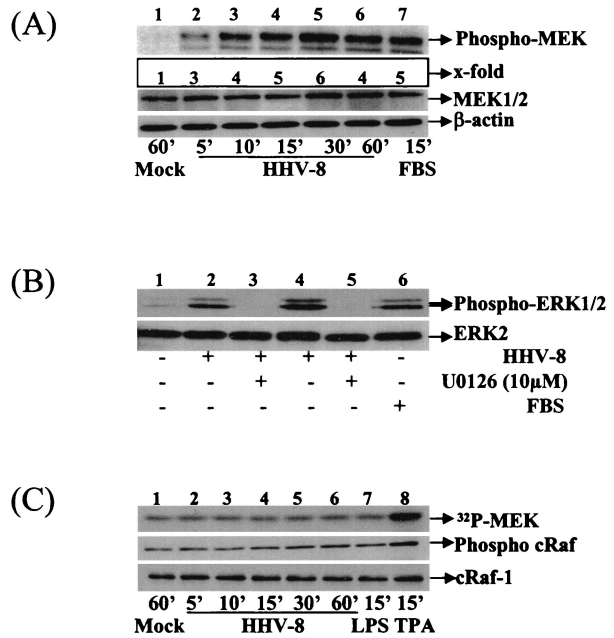

FIG. 4. HHV-8 induces MEK1/2 but not cRaf-1 in the target cells. (A) Kinetics of MEK1/2 induction. Serum-starved HFF cells were mock infected (lane 1), infected with HHV-8 (lanes 2 to 6), or treated with 20% FBS for the indicated times. Cell lysates were resolved by SDS–10% PAGE and probed with anti-phospho-MEK1/2 antibodies. Membranes were stripped and reprobed with anti-MEK1/2 antibodies (middle panel) or with anti-β actin antibodies (bottom panel). (B) Inhibition of MEK1/2 inhibits the ERK1/2 activity induced by HHV-8. Serum-starved HFF cells were mock infected (lane 1), infected with HHV-8 for 15 min (lane 2) or 30 min (lane 4), or incubated with 20% FBS for 15 min (lane 6). Cells were also preincubated with 10 μM MEK1/2 inhibitor U0126 for 1 h at 37°C and infected with virus in the presence of inhibitors for 15 and 30 min (lanes 3 and 5, respectively). Cell lysates were Western blotted and reacted with anti-phospho-ERK1/2 antibodies (top panel) or with anti-ERK2 antibodies (bottom panel). (C) HHV-8 does not induce cRaf-1 in the target cells. Serum-starved HFF cells were mock infected (lane 1), infected with HHV-8 (lanes 2 to 6), or treated with LPS (1 μg/ml; lane 7) or TPA (10 nM; lane 8) for the indicated times. Lysates were either immunoprecipitated with total cRaf-1 antibody and subjected to a kinase assay with MEK as substrate (top panel) or used for Western analysis with either phospho-cRaf-1 or total cRaf-1 antibody (middle and lower panels, respectively).

MAPK. No significant change in the phosphorylation of p38 was observed in HFF cells during 60 min of HHV-8 infection (Fig. 3E, lanes 2 to 5). The p38-MAPK was also not activated in HHV-8-infected HMVEC-d and 293 cells (data not shown). In contrast, HFF cells treated with 0.5 M sorbitol induced a fivefold activation of p38-MAPK by 5 min, which was sustained for 15 min and reached the background level by 30 min (Fig. 3E, lanes 6 to 8). These results suggested that HHV-8 preferentially induced the MAPK-ERK1/2 pathway and demonstrated the specificity of ERK induced by HHV-8.

MEK1/2 is an upstream inducer of HHV-8 activated ERK1/2 pathway. Since MEK1/2 is an upstream kinase that induces ERK1/2 (30), we used phosphorylation-specific antibodies to examine the MEK1/2 induction in HHV-8-infected cells. Compared to the mock-infected HFF cells (Fig. 4A, top panel, lane 1), phosphorylation of MEK1/2 in the infected cells increased in a time-dependent manner (Fig. 4A, top panel, lanes 2 to 6) from twofold at 5 min to a peak activation of fivefold at 30 min after HHV-8 infection. The MEK1/2 activity began to drop at 60 min (Fig. 4A, top panel, lane 6) and reached the background at 90 min (data not shown). In contrast, the total MEK or β-actin levels remained unaffected (Fig. 4A, middle and bottom panels, respectively).

Since the kinetics of MEK1/2 activation correlated well with ERK1/2 induction kinetics, to determine whether MEK1/2 is an upstream inducer of ERK-MAPK activated during the early stage of HHV-8 infection, HFF cells were treated with different concentrations of U0126 for 1 h at 37°C and infected with HHV-8 in the presence of U0126. U0126 is a potent and specific covalent binding inhibitor of MEK1/2 and shows little, if any, effect on the kinase activities of PKC, Abl, cRaf-1, MEKK, ERK, JNK, MKK-3, MKK-4/SEK, MKK-6, Cdk2, or Cdk4 (20). Lysates collected at 15 or 30 min postinfection were tested in a Western blot analysis with phopho-ERK1/2 antibodies and, at 10 μM concentrations, U0126 totally abolished the HHV-8-induced ERK phosphorylation (Fig. 4B, top panel, lanes 2 to 5). U0126 inhibited only the phosphorylation of ERK without affecting the total ERK levels (Fig. 4B, bottom panel, lanes 1 to 5). These results demonstrated that HHV-8 activation of ERK1/2 is dependent on MEK1/2 kinase activity and suggested that MEK1/2 is an upstream inducer of the HHV-8-activated ERK1/2 pathway.

cRaf-1 is not an upstream inducer of MEK1/2 involved in the HHV-8-activated ERK1/2 pathway. Since cRaf-1 is a well-described MAPKKK upstream activator of MEK1/2 (30), we evaluated the activation of cRaf-1 by HHV-8. In vitro kinase assays were performed with immunoprecipitated cRaf-1 by using polyhistidine-tagged-MEK as a substrate. There was no significant activation of cRaf-1 in HFF cells during the 60 min of HHV-8 infection (Fig. 4C, top panel, lanes 1 to 6). This was also confirmed by phospho c-Raf-1 antibodies (Fig. 4C, middle panel, lanes 1 to 6). The total cRaf-1 levels remained unaffected (Fig. 4C, bottom panel). Lack of cRaf-1 activation was also seen in HHV-8-infected HMVEC-d cells (data not shown). Similar to the earlier report (38), LPS (1 μg/ml) did not activate the cRaf-1 (Fig. 4C, lane 7, top and middle panel); however, LPS induced the ERK activation both in HFF and HMVEC-d cells (data not shown). In contrast, cells incubated for 15 min with a 10 nM concentration of TPA induced cRaf-1 activation (Fig. 4C, lane 8, top and middle panels). These results suggested that HHV-8-induced MEK1/2 and ERK1/2 activation was not dependent upon cRaf-1 induction.

HHV-8 induces the PKC-ζ activation during the early stage of infection. Enzymes of the PKC family, a component of focal adhesion, have been implicated in the actin cytoskeleton reorganization (28). Activation of atypical PKC isoenzymes λ and ζ induces the enhanced tyrosine phosphorylation of $pp125^{FAK}$ (54) and mediates Ras and Rac-1-dependent actin reorganization (25, 60). Further, ERK is activated in vivo by both conventional α, β, and γ isoforms of PKC and by the atypical isoforms ζ and λ (8). Studies addressing the role of PKC isoforms in the activation of cRaf-1, MEK, and ERK show that both PKC-α and PKC-ε activate cRaf-1 in vivo (10). In contrast, PKC-ζ did not activate cRaf-1 but did activate MEK1/2 and consequently ERK1/2 (52, 55). PKC-ζ could be activated in vitro by PtdIns-3,4,5-P_3, the lipid product of PI 3-kinase (26,

39). Since our results suggested the noninvolvement of cRaf-1 in the MEK/ERK activation by HHV-8, we hypothesized that focal adhesion components PI 3-kinase and PKC-ζ probably act as upstream candidates leading to MEK/ERK induction by HHV-8.

To determine the induction of PKC-ζ, HFF cells were infected with HHV-8, and in vitro kinase assays were performed with immunoprecipitated PKC-ζ by using MBP as a substrate. Western blot analysis detected comparable levels of PKC-ζ and ERK1/2 in HFF and HMVEC-d cells (data not shown). HHV-8 infection induced a rapid PKC-ζ phosphorylation in the target cells (Fig. 5A). Compared to mock infection, at 5, 10, 15, and 30 min after HHV-8 infection, ERK was activated by 2-, 3-, 2-, and 1.5-fold, respectively (Fig. 5A, top panel, lanes 2, 3, 4, and 5). HHV-8-induced PKC-ζ activation was comparable to the activation by LPS (1 μg/ml) and dPP (10 nM) (Fig. 5A, lanes 7 and 8, respectively), two known PKC-ζ activators (23, 38). Virus-induced activation represents a change in phosphorylation of PKC-ζ, since similar PKC-ζ/λ levels were detected by Western blot analyses with anti-PKC-ζ antibodies (Fig. 5A, bottom panel). HHV-8-mediated PKC-ζ activation was further confirmed by studies with antibodies against phosphorylated PKC-ζ (data not shown). Together with the data demonstrating the absence of cRaf-1 activation by HHV-8, these results suggest that MEK/ERK induction by HHV-8 is probably mediated by PKC-ζ.

PI 3-kinase-dependent PKC-ζ activation is the upstream event leading to MEK-ERK activation by HHV-8. To determine whether PI 3-kinase induction by HHV-8 is critical for the PKC-ζ, MEK1/2, and ERK activations, cells were preincubated for 1 h with PI 3-kinase inhibitors, wortmannin, and LY294002 and then infected with HHV-8 for 30 min in the presence of the inhibitors. PKC-ζ activity was quantitated by Western analysis with phospho-PKC-ζ antibodies. Both PI 3-kinase inhibitors abolished the HHV-8-induced PKC-ζ activities in a dose-dependent manner (Fig. 5B and C). Compared to untreated infected cells (Fig. 5B, lane 2), at a 100 nM concentration, wortmannin reduced the HHV-8-induced PKC-ζ activation by 85% (Fig. 5B, lane 3). At 200 and 500 nM concentrations, PKC-ζ activation reached the basal level (Fig. 5B, lanes 4 and 5). At a 25 μM concentration LY294002 reduced the HHV-8-induced PKC-ζ activation by 82% (Fig. 5C, lane 3), and at 50 and 100 μM concentrations PKC-ζ activation reached the basal level (Fig. 5C, lanes 4 and 5). The specificity of these reactions was demonstrated by the induction of PKC-ζ by 10 nM dPP (Fig. 5B, top panel, lane 6), by a lack of inhibition by dimethyl sulfoxide (DMSO; Fig. 5C, top panel, lane 6), and by the detection of similar PKC-ζ/λ levels by Western blot analyses with anti-PKC-ζ antibodies (Fig. 5B and C, bottom panels). PKC-ζ inhibition was also reproducible in the in vitro kinase assays with MBP as the substrate (data not shown). At the concentrations used here, wortmannin and LY294002 were not cytotoxic and did not affect the binding of radiolabeled HHV-8 to the target cells (data not shown). These results clearly indicated the requirement of PI 3-kinase activity for HHV-8-induced PKC-ζ activation.

To investigate the role of PI 3-kinase and PKC-ζ in HHV-8-induced ERK activation, cells were pretreated with wortmannin, LY294002, PKC pseudosubstrate-specific myr-ζ peptide, and control myr-α/β peptides for 1 h and then infected with HHV-8 for 30 min in the presence of these inhibitors. ERK activation as measured with phospho-ERK1/2 antibodies was inhibited by wortmannin, LY294002, and myr-ζ in a dose-dependent manner (Fig. 5D and E). At 100, 200, and 500 nM wortmannin concentrations, ERK phosphorylation was inhib-

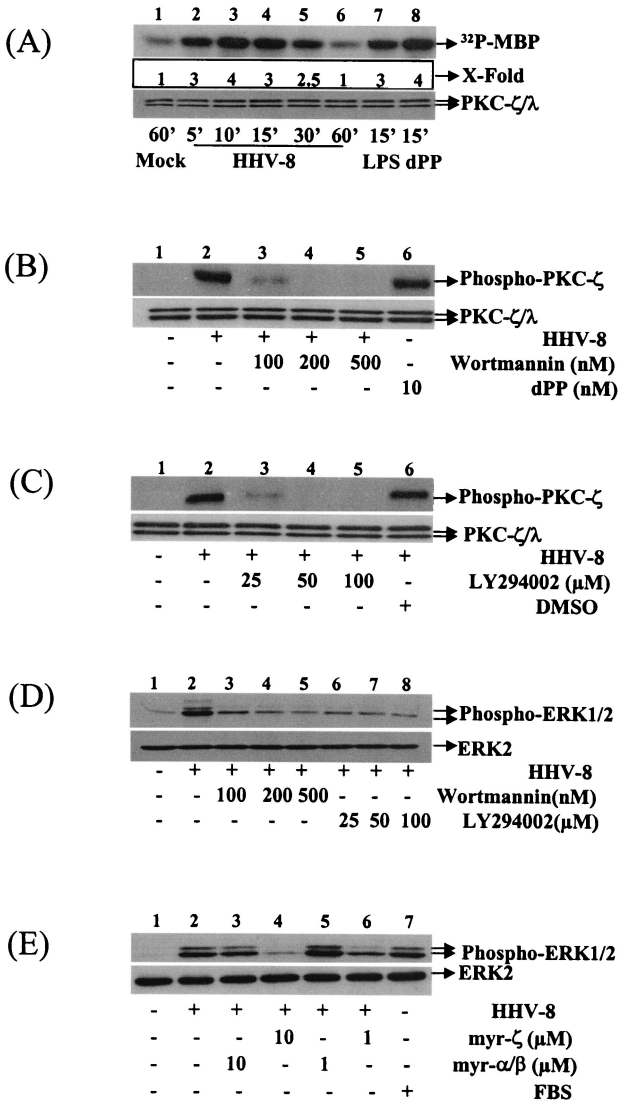

FIG. 5. Activation of ERK by HHV-8 is via the recruitment of PKC-ζ in a PI 3-kinase-dependent manner. (A) Kinetics of PKC-ζ activation by HHV-8. Lysates from mock-infected, HHV-8 infected, or known PKC-ζ inducer (LPS and dPP)-treated HFF cells were immunoprecipitated with anti-PKC-ζ antibodies and subjected to in vitro kinase assays with [γ-^{32}P]ATP and MBP as described for Fig. 3A (top panel). Western blotted immune complexes were tested with anti-PKC-ζ antibody (bottom panel). (B and C) PI 3-kinase inhibitors inhibit PKC-ζ activation by HHV-8. HFF cells were preincubated with different concentrations of the PI 3-kinase inhibitors wortmannin and LY294002 for 1 h at 37°C and infected with HHV-8 for 30 min. Lysates were tested in Western blot analysis with either phospho-PKC-ζ antibodies (top panel) or PKC-ζ antibody (lower panel). (D and E) PI 3-kinase and PKC-ζ inhibitors inhibit ERK1/2 activation. HFF cells were preincubated with PI 3-kinase or PKC-ζ inhibitors for 1 h at 37°C and then infected with HHV-8 for 30 min, and lysates tested in Western blots with phospho-ERK1/2 or total ERK2 (top and bottom panels, respectively).

ited by 70, 88, and 97%, respectively (Fig. 5D, lanes 3, 4, and 5). An ERK phosphorylation inhibition of 86, 90, and 96% was observed with 25, 50, and 100 μM concentrations of LY294002 (Fig. 5D, lanes 6 to 8). myr-ζ peptide at 10 and 1 μM concentrations reduced the HHV-8-induced ERK activation by 95 and 65%, respectively (Fig. 5E, lanes 4 and 6). No inhibition was seen with the control myr-α/β peptide (Fig. 5E, lanes 3 and 5) and with DMSO (data not shown). These results demonstrated that the focal adhesion components PI 3-kinase and PKC-ζ are critical mediators of HHV-8-induced ERK activation.

HHV-8 interaction with α3β1 integrin is one of the essential elements required for virus-induced ERK1/2 activation. HHV-8 binds and enters a variety of human cells (BCBL-1, BJAB, Raji, 293, HFF, HeLa, and endothelial cells), monkey cells (Vero and CV-1 cells), hamster cells (BHK-21 and CHO), and mouse cells (L) as shown by the detection of DNA, limited HHV-8 gene expression, and GFP expression (3). To verify the role of α3β1 in HHV-8 infectivity, we have previously used the CHO-B2 cells expressing low levels of endogenous α3 integrin transfected with human α3 integrin cDNA (CHO-B2-clone B3) (1). The human α3 integrin in transfected cells has been shown to form heterodimeric complexes with hamster β1 and is expressed on the plasma membranes, and fluorescence-activated cell sorting analyses have shown the expression of human α3 integrin in 95% of CHO-B2-B3 cells (1). The mean fluorescence intensity values for human α3 integrin in the B3 cells was 116, and the mean fluorescence intensity values for hamster α3 and β1 integrins in CHO cells were 3 and 60, respectively (1). The efficiency of infection in CHO-B2 cells was about 25-fold less than in HFF and HMVEC-d cells. However, the expression of human α3 integrin increased the susceptibility to HHV-8 infection, and CHO-B2-B3 cells were two to three times more susceptible to GFP–HHV-8 infectivity than the parental CHO-B2 cells (1). The permissiveness of these cells was also shown by the increased expression of ORF 73 protein (1). The increase in the level of HHV-8 infectivity was specifically blocked by the preincubation of cells with 2 μg of anti-human α3 antibodies/ml but not by the isotype-specific antibodies against human β4 integrin (1). The increased infectivity in these cells could be due to the ability of human α3-hamster β1 integrin to mimic a conformation resembling human α3β1 integrin. However, even though the radiolabeled HHV-8 binding to CHO cells mediated by HS-like molecules was comparable to HHV-8 binding to HFF and 293 cells, the virus infectivity in human α3-integrin expressing CHO-B2 cells was eightfold less than the infectivity in human cells. This suggests that the efficiency of HHV-8 entry in CHO cells may be dependent upon the density of α3β1 integrin, as well as other putative HHV-8 receptor(s). Nevertheless, these results indicated that the augmented HHV-8 infectivity was due to the expression of human α3 integrin and confirmed the role of α3β1 integrin in HHV-8 infectivity.

Engagement of α3β1 by HHV-8 activated the FAK, which was abolished significantly by preincubating the virus with soluble α3β1 integrin (1). PI 3-kinase is an important downstream effector of FAK, and PI 3-kinase induction essential for ERK1/2 activity was dependent upon HHV-8 interactions with α3β1 (Fig. 2). To verify the role of HHV-8–α3β1 interactions in the ERK1/2 activation, CHO-B2 cells expressing low levels

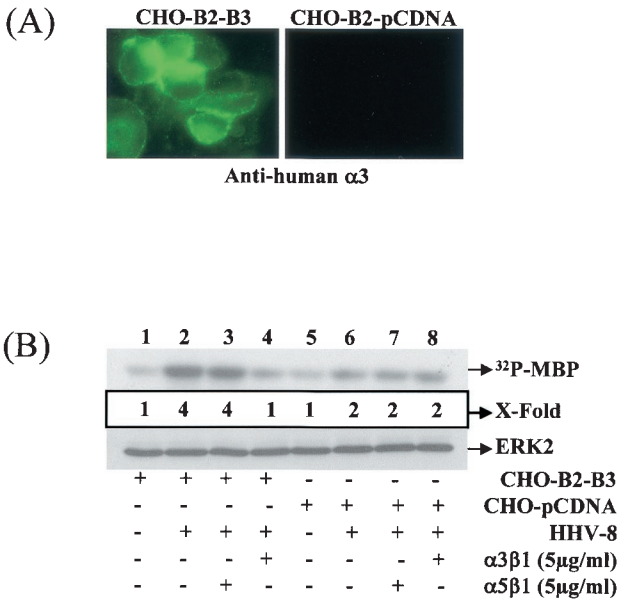

FIG. 6. Integrin α3β1 is one of the critical elements required for the signal induction by HHV-8. (A) Surface expression of human integrin α3 in CHO cells. CHO-B2 cells transfected with pCDNA3-human α3 integrin cDNA (CHO-B2-B3) or with control pCDNA3 plasmid (CHO-B2-pCDNA3) were grown in eight-well chamber slides, fixed with 0.1% paraformaldehyde, and tested by surface IFA staining with anti-human integrin α3 antibodies. (B) Induction of ERK1/2 by HHV-8 in human integrin α3 expressing CHO cells. Serum-starved CHO-B2-B3 and CHO-B2-pCDNA cells were either mock infected or infected with HHV-8 for 30 min. In parallel experiments, HHV-8 was incubated with 5 μg of soluble α3β1 or α5β1 integrin/ml for 1 h at 37°C before infection of the cells. ERK1/2 was immunoprecipitated and subjected to in vitro kinase assays (top panel) and immunoblot (bottom panel) as described for Fig. 3A. In the middle panel, ^{32}P-labeled MBP bands (top panel) were quantitated, and the ERK activity in mock-infected HFF cells was considered as "1" for comparison with the fold induction in the infected cells.

of endogenous α3 integrin transfected with human α3 integrin cDNA (CHO-B2-B3) or pCDNA3 vector DNA (CHO-B2-pCDNA) were used (67). The phenotype of these cells was confirmed by a surface IFA reaction with human α3 integrin antibodies (Fig. 6A). To determine whether the ability of HHV-8 to induce the ERK activity differs in the CHO-B2-B3 cells, an in vitro kinase assay was performed after a 15-min infection. HHV-8 induced a threefold-higher ERK1/2 activation in CHO-B2-B3 cells (Fig. 6B, top panel, lane 2) compared to the mock-infected CHO-B2-B3 (Fig. 6B, lane 1) or mock-infected CHO-B2-pCDNA (Fig. 6B, lane 5). DMEM containing 20% FBS induced ERK activation to similar levels in both cell types (data not shown), indicating that the observed difference with HHV-8 was not due to any other qualitative difference between these cells. The specificity of HHV-8-induced ERK activation via α3β1 was assessed by testing the ability of soluble integrins to inhibit HHV-8-mediated ERK induction. Soluble human α3β1 integrin at 5-μg/ml concentrations inhibited the HHV-8-mediated ERK induction in the human α3 integrin-expressing CHO-B2-B3 cells very efficiently (Fig. 6B, lane 4), and no effect was seen with α5β1 integrin (Fig. 6B, lane 3). Both human integrins could not block the onefold ERK induction seen in HHV-8-infected CHO-B2-

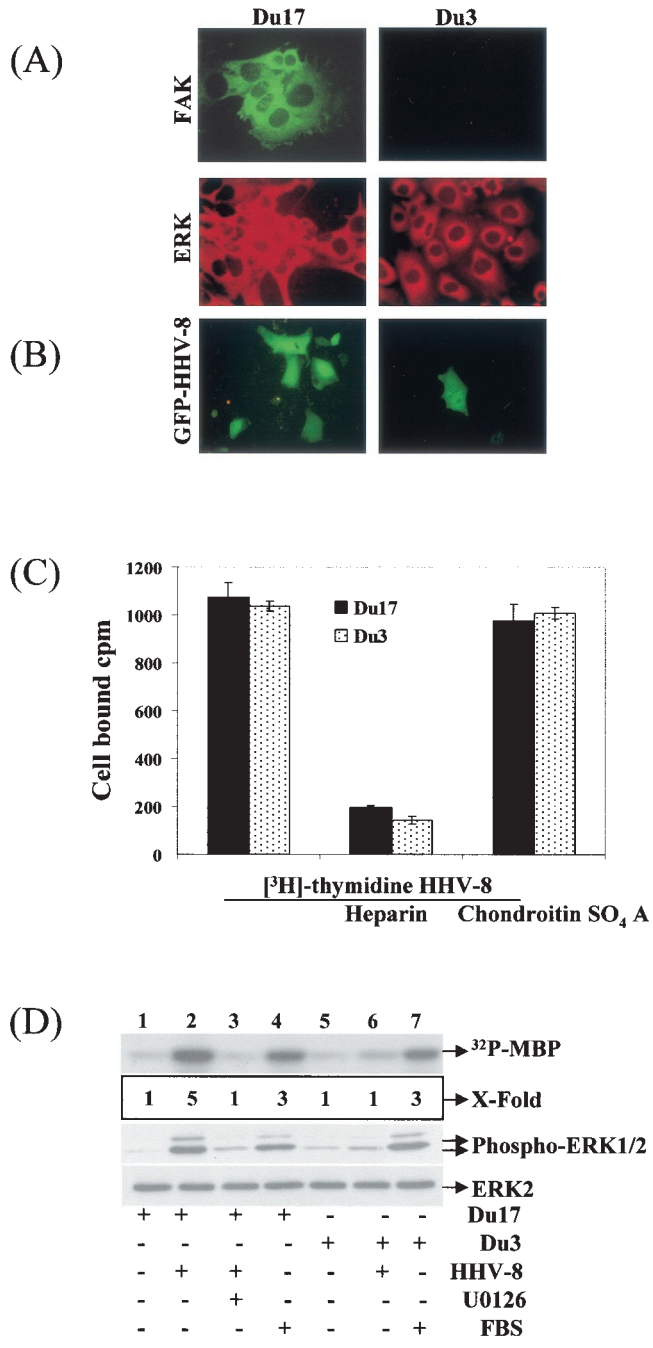

FIG. 7. FAK is essential for signal induction by HHV-8. (A) FAK and ERK expression in Du cells. Primary mouse embryonic fibroblasts dominant negative for FAK ($Du3^{-/-}$) and control FAK positive ($Du17^{+/+}$) were grown in chamber slides, washed, fixed with acetone, and reacted with anti-FAK or anti-ERK antibodies and fluorescein isothiocyanate- and rhodamine-labeled second antibodies. (B) FAK expression is essential for HHV-8 infectivity in the target cells. Du17/Du3 cells grown in eight-well chamber slides were infected with 100 μl of GFP–HHV-8, incubated at 37°C for 2 h, washed, and incubated with growth medium for 3 days. GFP-expressing cells were enumerated under a fluorescence microscope. Several areas of Du3 cells in a single chamber need to be searched to identify a single GFP-expressing cell. An average of eight GFP-expressing cells per well was seen in the Du3 cells infected with 100 μl of GFP–HHV-8 compared to 300 green fluorescent cells in the Du17 cells. (C) FAK expression is not essential for HHV-8 binding to the target cells. [^{3}H]thymidine labeled, purified HHV-8 (5,000 cpm) was mixed with 10 μg of heparin or chondrotin sulfate A/ml for 90 min at 4°C and then added to Du3 and Du17 cells. After incubation for 90 min at 4°C with the virus, cells were washed, lysed, and precipitated with trichloroacetic acid, and the cell-associated virus counts per minute (cpm) were counted. In the absence of heparin, ca. 21% of the input HHV-8 radioactivity became associated with the cells. Each reaction was done in triplicate, and each point represents the average ± the standard deviation of three experiments. (D) FAK expression is essential for ERK induction by HHV-8. Serum-starved Du17 and Du3 cells were either mock infected or infected with HHV-8 for 30 min. In another experiments, cells were incubated with U0126 for 1 h, and infected with HHV-8 for 30 min in the presence of inhibitor. ERK1/2 was immunoprecipitated and subjected to in vitro kinase assays (top panel), or total lysate was immunoblotted with anti-phospho-ERK1/2 antibodies (middle panel) or with total anti-ERK-2 antibodies (bottom panel) as described for Fig. 3A. ^{32}P-labeled MBP bands were quantitated, and the ERK activity in mock-infected cells was considered as "1" for comparison with infected cells.

pCDNA cells (Fig. 6B, lanes 7 and 8, respectively). The finding that these cells express low levels of endogenous hamster α3β1 integrin, as well as other integrin molecules, and since these cells could be still infected at very low efficiency by HHV-8 suggests that the onefold ERK induction by HHV-8 in the control cells may be due to the interactions of HHV-8 with the endogenous α3β1 integrin, other integrins, and/or other molecules. Since the expression of human α3 integrin increased the infectivity and the fold ERK activation in these cells, these results, taken together, suggested that HHV-8's interaction with α3β1 integrin is one of the essential elements required for the induction of the ERK1/2 signaling pathway.

FAK is one of the critical elements required for the HHV-8-induced ERK1/2 activation. Integrins have been suggested to initiate the ERK activation by a FAK-dependent mechanism via the association of FAK with Src and subsequent activation of the Ras/Raf/MAPK pathway (22) or by a FAK-independent mechanism via the association of β1 and αv integrins with the integral membrane protein caveolin and subsequent tyrosine phosphorylation of the adaptor protein Shc by the tyrosine kinase Fyn (65). Since HHV-8 interaction with α3β1 integrin activates FAK and since our results demonstrated the role of α3β1 integrin in HHV-8's induction of ERK1/2 signaling pathway, we next examined the role of FAK in HHV-8-mediated ERK activation. The FAK knockout mouse fibroblast cell line Du3 ($FAK^{-/-}$) and its parental line Du17 ($FAK^{+/+}$) (27) were used for infection with HHV-8. FAK was expressed only in Du17 cells and not in Du3 cells and, in contrast, both cells expressed similar levels of ERK (Fig. 7A). Western blot analysis with FAK- and ERK-specific antibodies also confirmed these results (data not shown). HHV-8 infection in Du17 cells was comparable to HFF cell infection. In contrast, GFP–HHV-8 infection was strikingly low in the Du3 cells, with ca. 40-fold less than that of Du17 cells (Fig. 7B). Several areas of Du3 cells in a single chamber need to be searched to identify a single GFP-expressing cell (Fig. 7B). An average of eight GFP-expressing cells per well was seen in the Du3 cells infected with 100 μl of GFP–HHV-8 compared to 300 green fluorescent cells in the Du17 cells. We have previously shown that cell surface HS is one of the initial contact molecules that HHV-8 uses to bind the target cells, which could be inhibited by preincubating virus with soluble heparin (3). [^{3}H]thymidine-

labeled HHV-8 bound both Du17 and Du3 cells with equal efficiency, which was inhibited by soluble heparin and not by chondroitin sulfate A (Fig. 7C). These results demonstrated that the reduced HHV-8 infectivity in Du3 cells was not due to the inability of virus to bind these cells but probably due to a block in the entry into these cells, thus suggesting a key role for FAK in HHV-8 infection. Whether the very low level of HHV-8 infection in the FAK-negative cells could be due to the activation of other FAK-related proteins such as Fak-related nonkinase, CAKβ, and PYK2/RAFTK or the activation of other pathways interlinking integrins to MAPK/ERK via alternative effectors needs to be studied.

ERK activation in Du17 and Du3 cells by HHV-8 was examined by in vitro kinase assay and phospho-ERK antibodies. Compared to mock-infected Du17 and Du3 cells (Fig. 7D, lanes 1 and 5, respectively), HHV-8 induced a fourfold increase in ERK activation in Du17 cells (Fig. 7D, lane 2) with only a minimal ERK activation in Du3 cells (Fig. 7D, lane 6). In contrast, 20% FBS in DMEM induced similar levels of ERK activity in both cell types (Fig. 7D, lanes 4 and 7), and the total ERK-2 levels remained unaffected between treatments in both cell types (Fig. 7D, lower panel). These results demonstrated the ability of cells to respond to other stimuli in similar fashion in a FAK-independent manner and suggested that the lack of ERK induction by HHV-8 in Du3 cells is probably attributed to the absence of FAK in these cells. ERK induction by HHV-8 in Du17 cells was inhibited to levels comparable to mock-infected cells (Fig. 7D, lane 1) by incubating cells with a 10 μM concentration of U0126 (Fig. 7D, lane 3), suggesting that the same hierarchy of MEK/ERK signaling pathway exists in this cell type. Taken together, these results suggested a critical role for FAK in the ERK activation by HHV-8.

HHV-8 induced cellular kinases are essential for HHV-8 infection of the target cells. Our studies clearly demonstrated the induction of the PI 3-kinase, PKC-ζ, MEK, ERK signaling pathways early during HHV-8 infection. In vitro infection of HFF and HMVEC-d cells with HHV-8 results only in the expression of its latent genes, and no lytic genes, such as the ORF 50 and other immediate early genes, were observed (61) (unpublished observations). Hence, to determine the role of these induced signaling cascades and the cellular kinases in HHV-8 infection, we used the GFP–HHV-8 infection system and examined the effects of various kinase inhibitors on GFP and ORF 73 expression. HFF cells were incubated with nontoxic doses of LY294002, wortmannin, myr-ζ, and U0126 at 37°C for 1 h before infection with GFP–HHV-8. GFP–HHV-8 infection of HFF cells only results in a latent infection without the expression of lytic cycle proteins and infectious progeny virus, and GFP-expressing cells thus represent infection by the input virus and not due to reinfection by the spread of replicating viruses from the infected cells (61). LY294002, myr-ζ, and U0126 inhibited the GFP–HHV-8 infection in a dose-dependent manner (Fig. 8A). Maximal inhibitions of 83, 88, and 92% were observed with U0126, myr-ζ, and LY294002 at 50, 10, and 200 μM concentrations, respectively. Similar results were also seen when ORF 73 expression was examined (data not shown). Although no inhibition was seen with myr-α/β and DMSO controls, a dose-dependent HHV-8 neutralization was observed with wortmannin (data not shown). Under these conditions, cell viability and the expression of other proteins were not affected (data not shown). These treatments did not affect the ability of radiolabeled virus to bind to the target cells (data not shown). These studies demonstrated that the activation of PI 3-kinase, PKC-ζ, and MEK are essential for HHV-8 entry and infection of the target cells.

To determine the importance of ERK in HHV-8 infection, an antisense oligonucleotide (AS-1/2) was used to deplete ERK1/2 in the target cells. Transfection of HFF cells with AS-1/2 at 0.05, 0.1, 0.2, and 0.5 μM reduced the ERK1/2 expression by 36, 58, 93 and, to basal level, respectively, at 48 h posttransfection (Fig. 8B, lanes 2 to 5). In contrast, the control SC-1/2 oligonucleotide (with scrambled sequence, but with the same nucleotide composition) did not have any effect even at a concentration of 0.5 μM (Fig. 8B, lane 6), suggesting that the inhibition of ERK1/2 expression by AS-1/2 was specific. Under these conditions, cell viability and expression of other proteins, such as β-actin, were not affected (Fig. 8B, lower panel). Similar results were also observed with HMVEC-d and 293 cells (data not shown). At the time point when ERK1/2 was maximally depleted (48 h), HFF cells were infected with GFP–HHV-8 and incubated for 3 days with the oligonucleotides before enumeration of the green fluorescent cells indicative of infection. At 0.2 and 0.5 μM concentrations, AS-1/2 inhibited HHV-8 infection by 60 to 63% and by 78 to 84%, respectively (Fig. 8C). These treatments did not affect the ability of the virus to bind to the target cells (data not shown). Concentrations of ≥0.5 μM were not attempted, since a ≥1 μM concentration of AS-1/2 was toxic to the cells (data not shown). No inhibitory effect was seen with control SC-1/2 oligonuclotide (Fig. 8C) or with Lipofectin used as a vehicle for delivery of oligonucleotides. These results demonstrated a role for the activation of cellular kinases in the infectious process of HHV-8.

PI 3-kinase inhibitors affect the internalization of HHV-8 DNA, and PKC-ζ, MEK, and ERK inhibitors affect at a post-viral entry stage of infection. Agents blocking the cellular kinases could block HHV-8 infection by interference at different stages of infection, viz., virus binding, virus internalization, release of capsid into the cytoplasm, transport of virus capsid to the cell nucleus, delivery viral DNA into the nucleus, and viral latent and/or lytic gene transcription. In the GFP–HHV-8 assay described above, the readings were taken after 3 days postinfection. Since HHV-8 infection of target HFF and HMVEC-d cells results only in latent infection with out the expression of viral lytic genes (unpublished observations), we could not examine the expression of viral immediate-early genes. Hence, to further determine the significance of neutralization of GFP–HHV-8 with kinase inhibitors without affecting the binding of radiolabeled virus to the target cells, we examined their effect on HHV-8 internalization.

HFF cells were incubated at 37°C for 1 h with neutralizing concentrations of wortmannin (300 nM), LY294002 (100 μM), myr-ζ (10 μM), U0126 (100 μM), and controls (DMSO; myr-α/β) or else transfected with AS1/2 (0.5 μM) and SC-1/2 for 48 h at 37°C. These cells were infected with ~5 MOI (ORF 73-IU) of GFP–HHV-8 in the presence of the inhibitors. After a washing step to remove the unbound virus, the cells were treated with trypsin-EDTA for 5 min to remove the bound but not internalized virus. Cells were subsequently washed, and the internalized HHV-8 DNA was isolated. Serial 10-fold dilutions

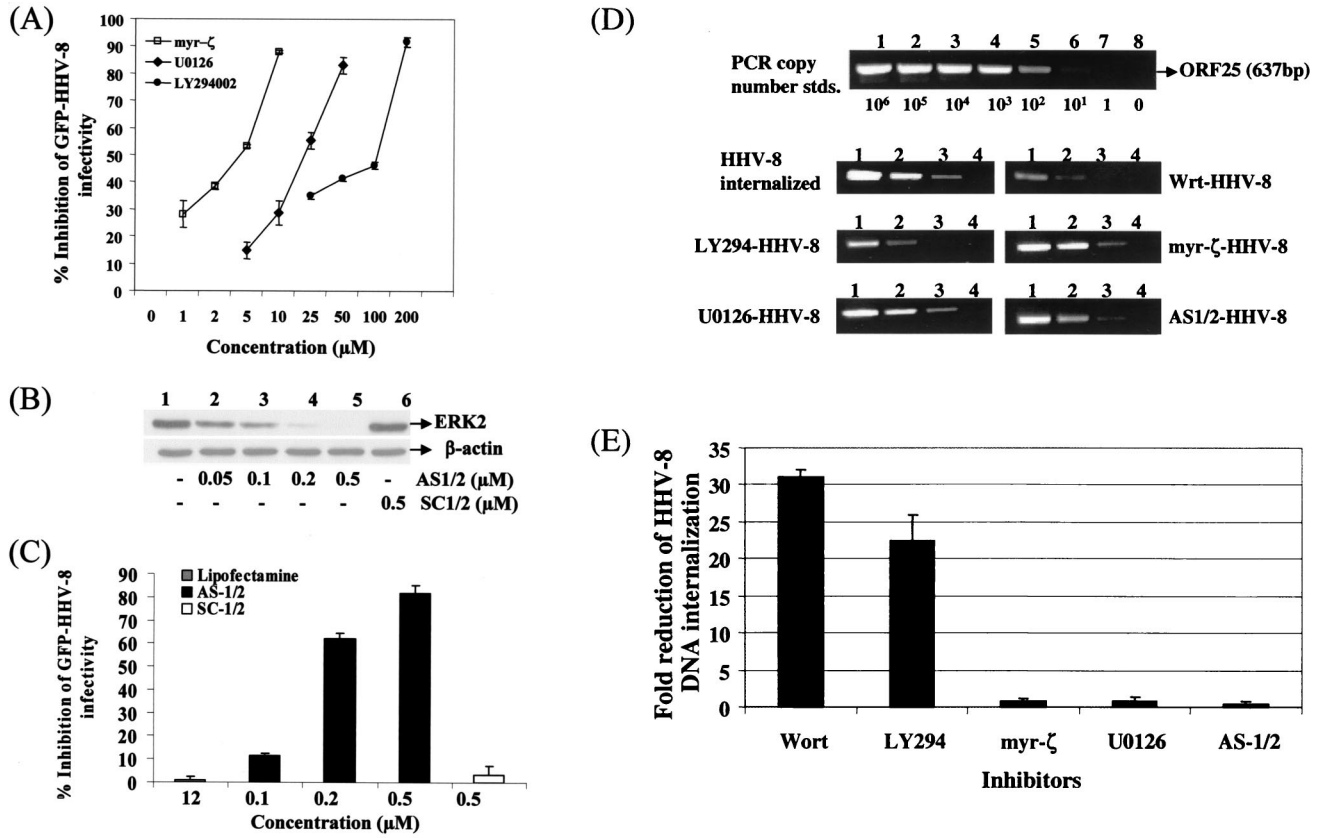

FIG. 8. Induction of cellular kinases by HHV-8 is essential for infectivity. (A) Neutralization of GFP–HHV-8 infectivity by inhibitors of PI 3-kinase, PKC-ζ, and MEK. HFF cell monolayers in eight-well chamber slides were incubated with DMEM containing different concentrations of nontoxic doses of LY294002 (PI 3-kinase inhibitor), myr-ζ (PKC-ζ specific inhibitory peptide), and U0126 (MEK inhibitor) at 37°C for 1 h before infection with GFP–HHV-8. After incubation for 2 h at 37°C with virus in the presence of inhibitors, cells were washed and further incubated with growth medium for 3 days at 37°C. Green fluorescent cells indicative of GFP–HHV-8 entry and infection were counted. In control wells, ca. 300 green fluorescent HFF cells per well were detected. Each reaction was done in triplicate and each point represents the average ± the standard deviation of three experiments. (B) ERK1/2 antisense oligonucleotide decreases the expression of ERK. HFF cells were transfected with AS-1/2 or control SC-1/2 oligonuclotides with Lipofectin at the indicated concentrations for 48 h. Cell lysates were analyzed by Western blot analysis with ERK2 antibodies (top panel) or β-actin (bottom panel) (C) ERK1/2 antisense oligonucleotide treatment reduces the infectivity of HHV-8. HFF cells were transfected with AS-1/2 or control SC-1/2 oligonucleotides for 48 h, infected with GFP–HHV-8 for 2 h at 37°C in the presence of oligonucleotides, washed, and incubated for 3 days at 37°C with growth medium containing the same concentration of oligonucleotides. Green fluorescent cells indicative of GFP–HHV-8 entry and infection were counted. In control wells, ca. 300 green fluorescent HFF cells per well were detected. Each reaction was done in triplicate, and each point represents the average ± the standard deviation of three experiments. (D) Effect of PI 3-kinase, PKC-ζ, MEK, and ERK inhibitors on HHV-8 internalization into the target cells. HFF cells were incubated at 37°C for 1 h with neutralizing concentrations of wortmannin (300 nM), LY294002 (100 μM), myr-ζ (10 μM), U0126 (100 μM), and controls (DMSO; myr-α/β) or transfected with AS-1/2 (0.5 μM), and SC-1/2 for 48 h at 37°C. Untreated HFF cells or HFF cells pretreated with various inhibitors were infected with GFP–HHV-8 at an MOI of ~5 73-IU for 2 h in the presence of the inhibitors. After infection, unbound HHV-8 was removed by washing the cells. Bound, noninternalized virus was removed by treating the cells with trypsin-EDTA for 5 min. Cells were washed, and the internalized viral DNA was isolated. To quantitate the HHV-8 PCR assays, a standard was prepared by cloning the ORF 25 PCR product into the pGEM-T vector and quantitated by UV absorption. Log_{10} dilutions of the standard DNA (10^6 to 10^1 copies) were amplified along with the virus stock and internalized DNA. The products were resolved on a 1.2% agarose gel stained with ethidium bromide, and the intensity was measured. The composite shows the PCR results from the copy number standard (top panel) and samples from HHV-8-infected untreated HFF cells and cells treated with the various kinase inhibitors. (E) Quantitation of the effect of kinase inhibitors on HHV-8 DNA internalization. The intensities of the bands in the agarose gels were scanned, and the copy numbers of internalized HHV-8 DNA in the absence and in the presence of kinase inhibitors were calculated by extrapolating the intensity of the band against the standard curve. Approximately 29% of the input vial DNA was internalized. Each reaction was done in triplicate, and each point represents the average ± the standard deviation of three experiments.

(500 to 0.5 ng) of total DNA from the cells and from the stock virus were subjected to PCR with HHV-8 ORF 25 (major capsid gene) primers amplifying a 637-bp fragment (Fig. 8D). Dilutions of copy standards (10^6 to 1^1 copies) of ORF 25 product were amplified in parallel (Fig. 8D). PCR products were resolved by agarose gel, the intensity of the bands was measured, and the copy number of internalized HHV-8 DNA was calculated against the standard curve (Fig. 8E). According to these estimations, ca. 29% (487,723 viral DNA copies) (Fig. 8D) of the input viral DNA (1,708,875 viral DNA copies) was internalized.

Treatment of HFF cells with PI 3-kinase inhibitors alone reduced the internalization of HHV-8 DNA significantly (Fig. 8D and E). A maximal inhibition was observed with wortman-

nin, which reduced the HHV-8 DNA internalization by 31-fold (Fig. 8E). Treatment with LY294002 reduced the internalization by 23-fold. Similar results were also observed in HMVEC-d cells (data not shown). In contrast, no significant inhibition was observed with myr-ζ, U0126, or AS-1/2 affecting PKC-ζ, MEK, and ERK, respectively (Fig. 8D and E). No inhibition was also seen with myr-α/β and DMSO controls (data not shown). These studies suggested that the inhibition of HHV-8 infectivity by the PI 3-kinase inhibitors probably due to a block at the entry stage of HHV-8 infection and thus suggest that the activation of PI 3-kinase plays a role in HHV-8 entry into the target cells. Inhibition of HHV-8 infectivity by the inhibitors of PKC-ζ, MEK and ERK without affecting the viral entry suggests a role for the activation of PKC-ζ and the MEK/ERK pathway at a post-viral entry stage of infection.

DISCUSSION

Several lines of evidence presented here demonstrate that during the initial stages of interaction with host cells, HHV-8 stimulates the integrin α3β1-FAK-dependent PI 3-kinase/PKC-ζ/MEK/ERK mitogenic signaling pathways essential for infection. The kinetics of induction suggest a requirement of this mitogenic pathway early during HHV-8 infection, a view which was supported by the significant neutralization of HHV-8 infection by inhibition of any of the member of this signal cascade. Similar to our findings, cell signaling pathways utilization during early stages of infection has been observed in other viruses. Simian virus 40 activates the primary response genes via a PKC-dependent pathway (16), whereas HIV rapidly induces the tyrosine phosphorylation of protein tyrosine kinase Pyk2 upon binding to CXCR4 or CCR5 (17, 66). Similarly, EBV, which binds to CD21, activates the resting B cells via a signaling pathway involving NF-κB (56), and human papillomavirus activates the Ras/MAPK pathway to induce cell proliferation by engaging the α6β4 integrin (44). The induction of signaling appears to be important for virus infectivity, since its blockade inhibited virus entry. For example, blocking simian virus 40 signaling by genistein did not affect virus binding, but virus uptake was severely reduced (16). Similarly, HIV entry was inhibited by pertussis toxin, which blocked the signaling from CCR5 and CXCR4 molecules (4). Only monophasic ERK activation with no activation beyond 60 min was seen in HHV-8 infection. Mitogenic signals induced by viruses exhibit a more sustained activation or biphasic activation, with the second phase coinciding with viral genome synthesis (34, 36).

Activation of MAPK by HHV-8 is not an unique event since HIV-1 (68), Borna disease virus (45), visna virus (7), and coxsackie B3 virus (34) have been shown to induce the MAPK pathway. However, our results suggest that HHV-8 induces a divergence of the MAPK cascade, since the commonly activated cRaf-1 was not induced. Most of the growth factors and other agonists are known to induce a Ras-mediated activation of Raf/MEK/ERK cascade (58). In contrast, insulin and LPS induce PI 3-kinase- and PKC-ζ-mediated ERK induction by directly activating MEK (38, 49). Respiratory syncytial virus activates ERK in cRaf-1-dependent and -independent ways (38). LPS mediates ERK signaling via Toll-like receptors (38), as well as by a Ras-independent ERK signaling via inhibitory protein G-coupled receptor (58). The absence of LPS contamination in our virus preparations, the failure of HHV-8 to induce the p38-MAPK pathway stimulated by LPS, the inhibition of signaling pathway by preincubating virus with anti-gB antibodies, and the requirement of α3β1 integrin and FAK by HHV-8 for signal induction clearly demonstrated the specificity of integrin-associated divergent mitogenic pathway activated by HHV-8 infection.

The ability of soluble human α3β1 integrin to block the ERK induction by HHV-8 and studies with CHO cells clearly indicate that ERK signaling induced by HHV-8 is at least in part mediated via α3β1 integrin. Although integrin α3β1 lacks an intracellular catalytic domain, its association with a cytoplasmic tyrosine kinase is responsible for initiating the outside-in signaling pathways (14). Three models have been proposed to explain the mechanism of integrin-mediated activation of the MAPK cascade. In the first model, integrin ligation leads to Src and FAK activation, Grb2 binding to FAK, and membrane localization of the guanine nucleotide exchange factor SOS, which then promotes Ras and subsequent Raf/MAPK activation (51). In the second model, integrins activate the Ras/MAPK pathway via the tyrosine kinase Fyn and the adaptor protein Shc (65). The third model proposes a Ras-independent activation of ERK by integrins (13, 33). Inefficient HHV-8 infection of FAK-negative Du3 cells and efficient infection of FAK-positive Du17 cells underscore the key role played by FAK both in ERK activation and in infection. Together with the activation of FAK by HHV-8 entry and the ability of genistein to efficiently block HHV-8-induced FAK phosphorylation (1) and HHV-8 infection (unpublished observations), our studies suggest that HHV-8-induced mitogenic signaling closely resembles the first model without the activation of cRaf-1. Further work is in progress to decipher the mediators upstream of the PI 3-kinase and to identify the other potential focal adhesion components involved in the HHV-8-induced signaling cascade.

Early kinetics of the cellular signaling pathway and its activation by UV-inactivated HHV-8 suggest a role for virus binding and/or entry, but not viral gene expression, in this induction. Reduction of HHV-8-induced ERK activity by anti-gB antibodies (which does not block virus binding to the cells), ERK activation and infection in FAK-positive Du17 cells, and their absence in FAK-negative Du3 cells despite efficient virus binding strongly indicate the involvement of a postattachment step of the virus entry pathway in the signal induction. HHV-8-encoded proteins such as v-cyclin, K12 (kaposin), v-GCR, K1, and K15 interact with several cellular signal transduction proteins (15, 57). However, a HHV-8 envelope association of these proteins has not been shown; v-cyclin and kaposin are expressed during the latent infection, and v-GPCR, K1, K15, and ORF 74 are expressed in the lytic cycle (50). In contrast, the glycoproteins gB, gPK8.1, gH, and gL are virion envelope-associated proteins and interact with cell surface receptors (2, 40, 64). The role of HHV-8 envelope glycoproteins in initiating the signaling cascades is under study.

What function might the rapid activation of the PI 3-kinase/PKC-ζ/MEK/ERK mitogenic signaling cascade serve during the initial stages of HHV-8 infection? Ligand mimicry is an opportunistic mechanism by which microbes subvert host signaling molecules for their entry into the host cells (9, 32, 62). HHV-8 probably takes advantage of the preexisting signaling

pathways to promote its entry into the target cells and to modulate a cellular state facilitating infection. Some alpha- and betaherpesviruses deliver their DNA-containing capsids into the cells by fusing their virion envelope with the plasma membrane. In contrast, in a manner similar to that of simian virus 40 (5) and γ1-EBV (42), γ2–HHV-8 enters via large endocytic vesicles in the human B-cell line BJAB (3), in HFF cells, and in endothelial cells (unpublished data). This is an exciting observation, since HHV-8 utilizes the α3β1 integrin as one of the entry receptors for its infectivity and activates FAK, which is intimately associated with the assembly of cytoskeleton and endocytosis. Receptor-mediated endocytosis and signaling pathways are interlinked and depend upon one another (37). In contrast to the earlier concept that endocytosis is a way to attenuate ligand-activated responses, recent studies suggest that signaling continues in the endocytic pathway and endocytosis plays a role in the activation and propagation of signaling pathways such as PI 3-kinase and ERK1/2 and vice versa (37).

A role for the activation of cellular kinases in the infectious process of HHV-8 was demonstrated by the reduction of infectivity by inhibitors specific for PI 3-kinase, PKC-ζ, MEK, and ERK kinase. Further studies are required to decipher the link between cellular kinases and the stages of virus infection. Our studies show that HHV-8 interaction with cells induces the polymerization of cortical actin filaments. Polymerized actin is suggested to provide the mechanical force that helps sever coated pit vesicles from the cell plasma membrane during endocytosis, as well as structural platforms that stabilize the half-lives of signaling molecules (18, 37). In addition to this initial role in the early steps of endocytosis, actin might participate in later events by propelling endocytic vesicles in the cytoplasm (19). Our data suggest that the inhibition of HHV-8 infectivity by the PI 3-kinase inhibitors is probably due to a block at the entry stage of HHV-8 infection and suggest a key role for the early induction of PI 3-kinase by HHV-8 in its entry. PI 3-kinase is an important downstream effector of FAK, which is activated either directly or through Src kinase via Ras (22). PI 3-kinase is involved in the activation of Rho-GTPases that are critical for the activation of Rac, Rho, Cdc4, and Rab5 involved in the modulation of actin dynamics, the formation of endocytic vesicles, and the fission of endocytic vesicles. Further work is in progress to decipher the PI 3-kinase-dependent activation of RhoGTPase, cdc42, Rho, and Rac and to define the role of the actin cytoskeleton in HHV-8 entry into target cells and in the release and movement of capsids in the cytoplasm. Since our studies suggest a role for the activation of the PKC-ζ, MEK, and ERK pathway at a post-viral entry stage of infection, further studies are essential to determine whether this pathway is essential for efficient transport of virus (capsid) to the cell nucleus, for delivery of viral DNA into the nucleus, and/or for viral latent and/or lytic gene transcription. Such studies and examination of the kinetics of viral ORF 73 (latent), ORF 50 (lytic switch) genes, and host gene expression by real-time PCR, and the stage of viral infection at which the signaling pathway inhibitors interfere are in progress.

What role does the rapid activation of the PI 3-kinase/PKC-ζ/MEK/ERK mitogenic signaling cascade during the initial stages of HHV-8 infection play in the association of HHV-8 in KS pathogenesis? In KS tissues, HHV-8 DNA is present in a latent form in the vascular endothelial and spindle cells (6). Only a limited set of HHV-8 genes, LANA1 (ORF 73), cyclin D (vCYC-(ORF72), vFLIP (ORF 71), and K12 is expressed in these cells (6). Despite the expression of these powerful viral proteins that can modulate cell growth (6, 53, 57), cells cultured from KS tumors grow for a limited number of passages, contain a mixture of cell types, depend upon growth factors, fail to grow in soft agar, and do not induce tumors in immunodeficient mice (21). The factors driving the KS tumor spindle cell growth, the inability of KS cells latently infected with HHV-8 to grow in cell culture, and the reasons for the loss of HHV-8 DNA within a few passages of KS cells are not known. Several lines of evidence, such as the detection of HHV-8 lytic cycle in KS lesion inflammatory cells, the reduced risk of KS by ganciclovir treatment that can inhibit HHV-8 replication (6), and the increased titer of antibodies against lytic cycle proteins in KS patients (6, 21) suggest a role for HHV-8 lytic replication in KS. Our present finding that HHV-8 induces integrin-mediated mitogenic signaling pathways and utilizes them for entry into the target cells may have important implications in the unique biology of KS lesions and in HHV-8's role in KS pathogenesis. HHV-8 interactions with β1 integrin, a molecule known to induce inflammatory cytokines and vascular endothelial growth factor via the induction of MEK-ERK1/2 (22), may stimulate the production of cytokines and/or growth factors in latently infected endothelial and adjacent cells, which in turn may stimulate the endothelial growth. A synergism may exist between latently infected endothelial cells and a lytic or abortive infection in B cells and other cells producing virus and/or viral proteins such as gB, interleukin-6, macrophage inflammatory protein 1 (MIP-1), and MIP-2, etc., which may control endothelial cell growth by an autocrine-parocrine loop. Since HHV-8 DNA is rarely found in in vitro cultures of KS spindle cells, if the latent HHV-8 episomes in spindle cells are not stably maintained, then the progression of a KS tumor in vivo could occur only by continuous interplay between the spindle cells and HHV-8 from the adjacent lytically infected reservoirs. Our model suggests a very complex interplay of various factors in the pathogenesis of KS and, if this model is proven correct, then these mechanisms would be unprecedented in tumor virology. Further studies are needed to examine the consequences of HHV-8-induced ERK and other signaling pathways in cells that are already programmed by the cell growth modulating HHV-8 latency-associated proteins and whether such interactions play a role in the establishment or maintenance of latent infection and/or the cellular proliferation of latently infected endothelial cells. A greater understanding of signaling pathways induced by HHV-8 may eventually lead to the development of novel therapies to control KS lesions.

ACKNOWLEDGMENTS

This study was supported in part by Public Health Service grants CA 75911 and 82056 to B.C. and grant P01 RR16443 to S.M.A. and by a University of Kansas Medical Center Biomedical Research Training program postdoctoral fellowship to P.P.N.

Technical help by Ling Zeng is greatly appreciated. We thank Jeffrey Vieira (Fred Hutchinson Cancer Research Center, Seattle, Wash.) for GFP–HHV-8-harboring BCBL-1 cells. We thank J. A. McDonald (Samuel C. Johnson Medical Research Center, Mayo Clinic, Scottsdale, Ariz.) for CHO-B2-B3 and CHO-B2-pCDNA cells; D. Ilic, Uni-

versity of California at San Francisco, for Du3 and Du17 cells; and Marilyn Smith for critically reading the manuscript.

REFERENCES

1. **Akula, S. M., N. P. Pramod, F.-Z. Wang, and B. Chandran.** 2002. Integrin α3β1(CD49c/28) is a cellular receptor for Kaposi's sarcoma-associated herpesvirus (KSHV/HHV-8) entry into the target cells. Cell **108:**407–419.
2. **Akula, S. M., N. P. Pramod, F. Z. Wang, and B. Chandran.** 2001. Human herpesvirus 8 envelope-associated glycoprotein B interacts with heparan sulfate-like moieties. Virology **284:**235–249.
3. **Akula, S. M., F.-Z. Wang, J. Vieira, and B. Chandran.** 2001. Human herpesvirus 8 interaction with target cells involves heparan sulfate. Virology **282:**245–255.
4. **Alfano, M., H. Schmidtmayerova, C. A. Amella, T. Pushkarsky, and M. Bukrinsky.** 1999. The B-oligomer of pertussis toxin deactivates CC chemokine receptor 5 and blocks entry of M-tropic HIV-1 strains. J. Exp. Med. **190:**597–605.
5. **Anderson, H. A., Y. Chen, and L. C. Norkin.** 1996. Bound simian virus 40 translocates to caveolin-enriched membrane domains, and its entry is inhibited by drugs that selectively disrupt caveolae. Mol. Biol. Cell **7:**1825–1834.
6. **Antman, K., and Y. Chang.** 2000. Kaposi's sarcoma. N. Engl. J. Med. **342:** 1027–1038.
7. **Barber, S. A., L. Bruett, B. R. Douglass, D. S. Herbst, M. C. Zink, and J. E. Clements.** 2002. Visna virus-induced activation of MAPK is required for virus replication and correlates with virus-induced neuropathology. J. Virol. **76:**817–828.
8. **Berra, E., M. T. Diaz-Meco, I. Dominguez, M. M. Municio, L. Sanz, J. Lozano, R. S. Chapkin, and J. Moscat.** 1993. Protein kinase C zeta isoform is critical for mitogenic signal transduction. Cell **74:**555–563.
9. **Bliska, J. B., J. E. Galan, and S. Falkow.** 1993. Signal transduction in the mammalian cell during bacterial attachment and entry. Cell **73:**903–920.
10. **Cai, H., U. Smola, V. Wixler, I. Eisenmann-Trappe, M. T. Diaz-Meco, J. Moscat, U. Rapp, and G. M. Cooper.** 1997. Role of DAG-regulated PKC isotypes in growth factor activation of the Raf-1 protein kinase. Mol. Cell. Biol. **17:**732–741.
11. **Cerimele, F., F. Curreli, S. Ely, A. E. Friedman-Kien, E. Cesarman, and O. Flore.** 2001. Kaposi's sarcoma associated herpesvirus can productively infect primary human keratinocytes and alter their growth properties. J. Virol. **75:**2435–2443.
12. **Chang, Y., E. Cesarman, M. S. Pessin, F. Lee, J. Culpepper, D. M. Knowles, and P. S. Moore.** 1994. Identification of herpesvirus-like DNA sequences in AIDS-associated Kaposi's sarcoma. Science **266:**1865–1869.
13. **Chen, Q., T. H. Lin, C. J. Der, and R. L. Juliano.** 1996. Integrin-mediated activation of MEK and mitogen-activated protein kinase is independent of Ras. J. Biol. Chem. **271:**18122–18127.
14. **Clark, E. A., and J. S. Brugge.** 1995. Integrins and signal transduction pathways: the road taken. Science **268:**233–239.
15. **Damania, B., J. K. Choi, and J. U. Jung.** 2000. Signaling activities of gammaherpesvirus membrane proteins. J. Virol. **74:**1593–1601.
16. **Dangoria, S., W. C. Breau, H. A. Anderson, D. M. Cishek, and L. C. Norkin.** 1996. Extracellular simian virus 40 induces an ERK/MAP kinase-independent signaling pathway that activates primary response genes and promotes virus entry. J. Gen. Virol. **77:**2173–2182.
17. **Davis, C. B., I. Dikic, D. Unutmaz, C. M. Hill, J. Arthos, M. A. Siani, D. A. Thompson, J. Schlessinger, and D. R. Littman.** 1997. Signal transduction due to HIV-1 envelope interactions with chemokine receptors CXCR4 or CCR5. J. Exp. Med. **186:**1793–1798.
18. **Di Fiore, P. P., and P. De Camilli.** 2001. Endocytosis and signaling: an inseparable partnership. Cell **106:**1–4.
19. **Dramsi, S., and P. Cossart.** 1998. Intracellular pathogens and the actin cytoskeleton. Annu. Rev. Cell Dev. Biol. **14:**137–166.
20. **Favata, M. F., K. Y. Horiuchi, E. J. Manos, A. J. Daulerio, D. A. Stradley, W. S. Feeser, D. E. Van Dyk, W. J. Pitts, R. A. Earl, F. Hobbs, R. A. Copeland, R. L. Magolda, P. A. Scherle, and J. M. Trzaskos.** 1998. Identification of a novel inhibitor of mitogen-activated protein kinase kinase. J. Biol. Chem. **273:**18623–18632.
21. **Ganem, D.** 1998. Human herpesvirus 8 and its role in the genesis of Kaposi's sarcoma. Curr. Clin. Top. Infect. Dis. **18:**237–251.
22. **Giancotti, F. G., and E. Ruoslahti.** 1999. Integrin signaling. Science **285:** 1028–1032.
23. **Gupta, S., S. Aggarwal, C. Kim, and S. Gollapudi.** 1994. Human immunodeficiency virus-1 recombinant gp120 induces changes in protein kinase C isozymes: a preliminary report. Int. J. Immunopharmacol. **16:**197–204.
24. **Hall, A.** 1998. Rho GTPases and the actin cytoskeleton. Science **279:**509–514.
25. **Hellbert, K., S. Kampfer, K. Maly, F. Hochholdinger, J. Mwanjewe, G. Baier, F. Uberall, and H. H. Grunicke.** 2000. Implication of atypical protein kinase C isozymes lambda and zeta in Ras-mediated reorganization of the actin cytoskeleton and cyclin D1-induction. Adv. Enzyme Regul. **40:**49–62.
26. **Herrera-Velit, P., K. L. Knutson, and N. E. Reiner.** 1997. Phosphatidylinositol 3-kinase-dependent activation of protein kinase C-ζ in bacterial lipopolysaccharide-treated human monocytes. J. Biol. Chem. **272:**16445–16452.
27. **Ilic, D., Y. Furuta, S. Kanazawa, N. Takeda, K. Sobue, N. Nakatsuji, S. Nomura, J. Fujimoto, M. Okada, and T. Yamamoto.** 1995. Reduced cell motility and enhanced focal adhesion contact formation in cells from FAK-deficient mice. Nature **377:**539–544.
28. **Keenan, C., and D. Kelleher.** 1998. Protein kinase C and the cytoskeleton. Cell Signal **10:**225–232.
29. **Koelle, D. M., M. L. Huang, B. Chandran, J. Vieira, M. Piepkorn, and L. Corey.** 1997. Frequent detection of Kaposi's sarcoma-associated herpesvirus (human herpesvirus 8) DNA in saliva of human immunodeficiency virus-infected men: clinical and immunologic correlates. J. Infect. Dis. **176:**94–102.
30. **Kolch, W.** 2000. Meaningful relationships: the regulation of the Ras/Raf/MEK/ERK pathway by protein interactions. Biochem. J. **351:**289–305.
31. **Kotani, K., K. Yonezawa, K. Hara, H. Ueda, Y. Kitamura, H. Sakaue, A. Ando, A. Chavanieu, B. Calas, F. Grigorescu, M. Nishiyama, M. D. Waterfield, and M. Kasuga.** 1994. Involvement of phosphoinositide 3-kinase in insulin- or IGF-1-induced membrane ruffling. EMBO J. **13:**2313–2321.
32. **Li, E., D. Stupack, G. M. Bokoch, and G. R. Nemerow.** 1998. Adenovirus endocytosis requires actin cytoskeleton reorganization mediated by Rho family GTPases. J. Virol. **72:**8806–8812.
33. **Lin, T. H., A. E. Aplin, Y. Shen, Q. Chen, M. Schaller, L. Romer, I. Aukhil, and R. L. Juliano.** 1997. Integrin-mediated activation of MAP kinase is independent of FAK: evidence for dual integrin signaling pathways in fibroblasts. J. Cell Biol. **136:**1385–1395.
34. **Luo, H., B. Yanagawa, J. Zhang, Z. Luo, M. Zhang, M. Esfandiarei, C. Carthy, J. E. Wilson, D. Yang, and B. M. McManus.** 2002. Coxsackievirus B3 replication is reduced by inhibition of the extracellular signal-regulated kinase (ERK) signaling pathway. J. Virol. **76:**3365–3373.
35. **Marion, P. L., J. M. Cullen, R. R. Azcarraga, M. J. Van Davelaar, and W. S. Robinson.** 1987. Experimental transmission ofduck hepatitis B virus to Pekin ducks and to domestic geese. Hepatology **7:**724–731.
36. **McLean, T. I., and S. L. Bachenheimer.** 1999. Activation of cJUN N-terminal kinase by herpes simplex virus type 1 enhances viral replication. J. Virol. **73:**8415–8426.
37. **McPherson, P. S., B. K. Kay, and N. K. Hussain.** 2001. Signaling on the endocytic pathway. Traffic **2:**375–384.
38. **Monick, M., J. Staber, K. Thomas, and G. Hunninghake.** 2001. Respiratory syncytial virus infection results in activation of multiple protein kinase C isoforms leading to activation of mitogen-activated protein kinase. J. Immunol. **166:**2681–2687.
39. **Nakanishi, H., K. A. Brewer, and J. H. Exton.** 1993. Activation of the zeta isozyme of protein kinase C by phosphatidylinositol 3,4,5-trisphosphate. J. Biol. Chem. **268:**13–16.
40. **Naranatt, P. P., S. M. Akula, and B. Chandran.** 2002. Characterization of γ2-human herpesvirus-8 glycoproteins gH and gL. Arch. Virol. **147:**1349–1370.
41. **Neipel, F., J. C. Albrecht, and B. Fleckenstein.** 1997. Cell-homologous genes in the Kaposi's sarcoma-associated rhadinovirus human herpesvirus 8: determinants of its pathogenicity? J. Virol. **71:**4187–4192.
42. **Nemerow, G. R., and N. R. Cooper.** 1984. Early events in the infection of human lymphocytes by Epstein-Barr virus: the internalization process. Virology **132:**186–198.
43. **Nishiyama, T., T. Sasaki, K. Takaishi, M. Kato, H. Yaku, K. Araki, Y. Matsuura, and Y. Takai.** 1994. Rac p21 is involved in insulin-induced membrane ruffling and *rho* p21 is involved in hepatocyte growth factor- and 12-*O*-tetradecanoylphorbol-13-acetate (TPA)-induced membrane ruffling in KB cells. Mol. Cell. Biol. **14:**2247–2256.
44. **Payne, E., M. R. Bowles, A. Don, J. F. Hancock, and N. A. McMillan.** 2001. Human papillomavirus type 6b virus-like particles are able to activate the Ras-MAP kinase pathway and induce cell proliferation. J. Virol. **75:**4150–4157.
45. **Planz, O., S. Pleschka, and S. Ludwig.** 2001. MEK-specific inhibitor U0126 blocks spread of Borna disease virus in cultured cells. J. Virol. **75:**4871–4877.
46. **Renne, R., D. Blackbourn, D. Whitby, J. Levy, and D. Ganem.** 1998. Limited transmission of Kaposi's sarcoma-associated herpesvirus in cultured cells. J. Virol. **72:**5182–5188.
47. **Renshaw, M. W., D. Toksoz, and M. A. Schwartz.** 1996. Involvement of the small GTPase Rho in integrin-mediated activation of mitogen-activated protein kinase. J. Biol. Chem. **271:**21691–21694.
48. **Russo, J. J., R. A. Bohenzky, M. C. Chien, J. Chen, M. Yan, D. Maddalena, J. P. Parry, D. Peruzzi, I. S. Edelmen, Y. Chang, and P. S. Moore.** 1996. Nucleotide sequence of the Kaposi's sarcoma-associated herpesvirus (HHV-8). Proc. Natl. Acad. Sci. USA **93:**14862–14867.
49. **Sajan, M. P., M. L. Standaert, G. Bandyopadhyay, M. J. Quon, T. R. Burke, Jr., and R. V. Farese.** 1999. Protein kinase C-ζ and phosphoinositide-dependent protein kinase-1 are required for insulin-induced activation of ERK in rat adipocytes. J. Biol. Chem. **274:**30495–30500.
50. **Sarid, R., O. Flore, R. A. Bohenzky, Y. Chang, and P. S. Moore.** 1998. Transcription mapping of the Kaposi's sarcoma-associated herpesvirus (HHV-8) genome in a body cavity-based lymphoma cell line (BC-1). J. Virol. **72:**1005–1012.
51. **Schlaepfer, D. D., and T. Hunter.** 1997. Focal adhesion kinase overexpression enhances Ras-dependent integrin signaling to ERK2/mitogen-activated

protein kinase through interactions with and activation of c-Src. J. Biol. Chem. **272:**13189–13195.
52. **Schonwasser, D. C., R. M. Marais, C. J. Marshall, and P. J. Parker.** 1998. Activation of the mitogen-activated protein kinase/extracellular signal-regulated kinase pathway by conventional, novel, and atypical protein kinase C isotypes. Mol. Cell. Biol. **18:**790–798.
53. **Schulz, T. F., Y. Chang, and P. S. Moore.** 1998. Kaposi's sarcoma-associated herpesvirus (human herpesvirus 8), p. 87–134. *In* D. J. McCance (ed.), Human tumor viruses. ASM, Washington, D.C.
54. **Smith-Sinnett, J., I. Zachary, A. M. Valverde, and E. Rozengurt.** 1993. Bombesin stimulation of p125 focal adhesion kinase tyrosine phosphorylation. J. Biol. Chem. **268:**14261–14268.
55. **Sozeri, O., K. Vollmer, M. Liyanage, D. Frith, G. Kour, G. E. Mark, and S. Stabel.** 1992. Activation of the c-Raf protein kinase by protein kinase C phosphorylation. Oncogene **7:**2259–2262.
56. **Sugano, N., W. Chen, M. L. Roberts, and N. R. Cooper.** 1997. Epstein-Barr virus binding to CD21 activates the initial viral promoter via NF-κB induction. J. Exp. Med. **186:**731–737.
57. **Swanton, C., and N. Jones.** 2001. Strategies in subversion: deregulation of the mammalian cell cycle by viral gene products. Int. J. Exp. Pathol. **82:**3–13.
58. **Takeda, H., T. Matozaki, T. Takada, T. Noguchi, T. Yamao, M. Tsuda, F. Ochi, K. Fukunaga, K. Inagaki, and M. Kasuga.** 1999. PI 3-kinase gamma and protein kinase C-ζ mediate RAS-independent activation of MAP kinase by a Gi protein-coupled receptor. EMBO J. **18:**386–395.
59. **Triantafilou, K., Y. Takada, and M. Triantafilou.** 2001. Mechanisms of integrin-mediated virus attachment and internalization process. Crit. Rev. Immunol. **21:**311–322.
60. **Uberall, F., K. Hellbert, S. Kampfer, K. Maly, A. Villunger, M. Spitaler, J. Mwanjewe, G. Baier-Bitterlich, G. Baier, and H. H. Grunicke.** 1999. Evidence that atypical protein kinase C-λ and atypical protein kinase C-ζ participate in Ras-mediated reorganization of the F-actin cytoskeleton. J. Cell Biol. **144:**413–425.
61. **Vieira, J., P. O'Hearn, L. Kimball, B. Chandran, and L. Corey.** 2001. Activation of KSHV (HHV-8) lytic replication by human cytomegalovirus. J. Virol. **75:**1378–1386.
62. **Virji, M.** 1996. Microbial utilization of human signaling molecules. Microbiology **142:**3319–3336.
63. **Walker, E. H., M. E. Pacold, O. Perisic, L. Stephens, P. T. Hawkins, M. P. Wymann, and R. L. Williams.** 2000. Structural determinants of phosphoinositide 3-kinase inhibition by wortmannin, LY294002, quercetin, myricetin, and staurosporine. Mol. Cell **6:**909–919.
64. **Wang, F.-Z., S. M. Akula, N. P. Pramod, L. Zeng, and B. Chandran.** 2001. Human herpesvirus 8 envelope glycoprotein K8.1A interaction with the target cells involves heparin sulfate. J. Virol. **75:**7517–7527.
65. **Wary, K. K., A. Mariotti, C. Zurzolo, and F. G. Giancotti.** 1998. A requirement for caveolin-1 and associated kinase Fyn in integrin signaling and anchorage-dependent cell growth. Cell **94:**625–634.
66. **Weissman, D., R. L. Rabin, J. Arthos, A. Rubbert, M. Dybul, R. Swofford, S. Venkatesan, J. M. Farber, and A. S. Fauci.** 1997. Macrophage-tropic HIV and SIV envelope proteins induce a signal through the CCR5 chemokine receptor. Nature **389:**981–985.
67. **Wu, C., A. E. Chung, and J. A. McDonald.** 1995. A novel role for α3β1 integrins in extracellular matrix assembly. J. Cell Sci. **108:**2511–2523.
68. **Yang, X., and D. Gabuzda.** 1999. Regulation of human immunodeficiency virus type 1 infectivity by the ERK mitogen-activated protein kinase signaling pathway. J. Virol. **73:**3460–3466.
69. **Zhu, L., V. Puri, and B. Chandran.** 1999. Characterization of human herpesvirus-8 K8.1 A/B glycoproteins by monoclonal antibodies. Virology **262:** 237–249.